

# Novel Benzylidene-9(10*H*)-anthracenones as Highly Active Antimicrotubule Agents. Synthesis, Antiproliferative Activity, and Inhibition of Tubulin Polymerization

Helge Prinz,<sup>\*,†</sup> Yukihito Ishii,<sup>‡</sup> Takeo Hirano,<sup>‡</sup> Thomas Stoiber,<sup>§</sup> Juan A. Camacho Gomez,<sup>§</sup> Peter Schmidt,<sup>||</sup> Heiko Düssmann,<sup>⊥</sup> Angelika M. Burger,<sup>⊗</sup> Jochen H. M. Prehn,<sup>⊥</sup> Eckhard G. Günther,<sup>||</sup> Eberhard Unger,<sup>§</sup> and Kazuo Umezawa<sup>‡</sup>

*Institute of Pharmaceutical and Medicinal Chemistry, Westphalian Wilhelms-University, Hittorfstrasse 58-62, D-48149 Münster, Germany, Zentaris AG, Weismüllerstrasse 45, D-60314 Frankfurt, Germany, Oncotest GmbH, Am Flughafen 12-14, D-79108 Freiburg, Germany, Department of Applied Chemistry, Faculty of Science and Technology, Keio University, 3-14-1 Hiyoshi, Kohoku-ku, Yokohama 223-0061, Japan, Interdisciplinary Center for Clinical Research, Research Group "Apoptosis and Cell Death", Westphalian Wilhelms-University, Röntgenstrasse 21, D-48149 Münster, Germany, and Institute of Molecular Biotechnology e.V., Department of Molecular Cytology – Electron Microscopy, Beutenbergstrasse 11, D-07708 Jena, Germany*

Received January 15, 2003

A novel series of 10-benzylidene-9(10*H*)-anthracenones and 10-(phenylmethyl)-9(10*H*)-anthracenones were synthesized and evaluated for antiproliferative activity in an assay based on K562 leukemia cells. The 3-hydroxy-4-methoxybenzylidene analogue **9h** was found to be the most active compound (IC<sub>50</sub> K562: 20 nM). Structure–activity relationships are also considered. The highly active compound **9h** and the 2,4-dimethoxy-3-hydroxybenzylidene analogue **9l** were tested against five tumor cell lines using the XTT assay, including multidrug resistant phenotypes. Induction of cell death in a variety of tumor cell lines was determined in a monolayer assay using propidium iodide. Noteworthy, all compounds within the series induced elongations in K562 cells similar to vinblastine-treated cells. The effect of the lead compound **9h** on K562 cell growth was associated with cell cycle arrest in G2/M. Concentrations for 50% KB/HeLa cells arrested in G2/M after treatment with **9h** and **9l** were determined and found to be in the range of 0.2 μM. Additionally, we monitored the dose dependent caspase-3-like protease activity in K562 cells and MCF-7/Casp-3 cells treated with **9h**, indicating induction of apoptosis. Western blotting analysis demonstrated that **9h** caused a shift in tubulin concentration from the polymerized state found in the cell pellet to the unpolymerized state found in the cell supernatant. Seven compounds strongly inhibited tubulin polymerization with activities higher or comparable to those of the reference compounds such as colchicine, podophyllotoxin, and nocodazole. In general, the antiproliferative activity correlated with inhibition of tubulin polymerization. The most active compounds strongly displaced [<sup>3</sup>H]colchicine from its binding site in the tubulin, yielding IC<sub>50</sub> values 3- to 4-fold lower than that of colchicine. The novel benzylidene-9(10*H*)-anthracenones described in the present study constitute an interesting group of highly active and easily accessible antimitotic agents that inhibit tubulin polymerization.

## Introduction

Attacking the microtubule system is a common strategy to inhibit tumor cell proliferation. The importance of microtubules for cellular life and especially mitosis as well as for the induction and progression of apoptosis makes them one of the most prominent targets for the development of anticancer agents and for the treatment of solid tumors.<sup>1–3</sup> Microtubules are hollow tubes found in almost all eukaryotic cell types. They are directly involved in a variety of cellular functions, such as

mitosis and cell replication, cell movement, cell maintenance, and cell shape, as well as transport of organelles inside the cell. Tubulin together with its isotypes is the major building block of microtubules and exists as a heterodimer of α- and β-tubulin. Both globular polypeptides have a molecular mass between 50 and 55 kDa and combine stoichiometrically. This heterodimer binds two molecules of guanosine triphosphate (GTP), which are involved in tubulin functions. By interfering with tubulin assembly, for example by inhibiting tubulin polymerization or causing depolymerization upon binding to tubulin, novel compounds provide new perspectives for the inhibition of tumor cell growth and suppression of cancer. Meanwhile, numerous antimitotic agents displaying a wide structural diversity have been found to affect microtubule dynamics. Almost all of them interact with the α/β-tubulin dimer, rather than microtubule-associated proteins (MAPs) or other proteins involved in microtubule func-

\* To whom correspondence should be addressed. Tel: +49 251-8333325. Fax: +49 251-8332144. E-mail: prinzh@uni-muenster.de.

† Institute of Pharmaceutical and Medicinal Chemistry, Westphalian Wilhelms University.

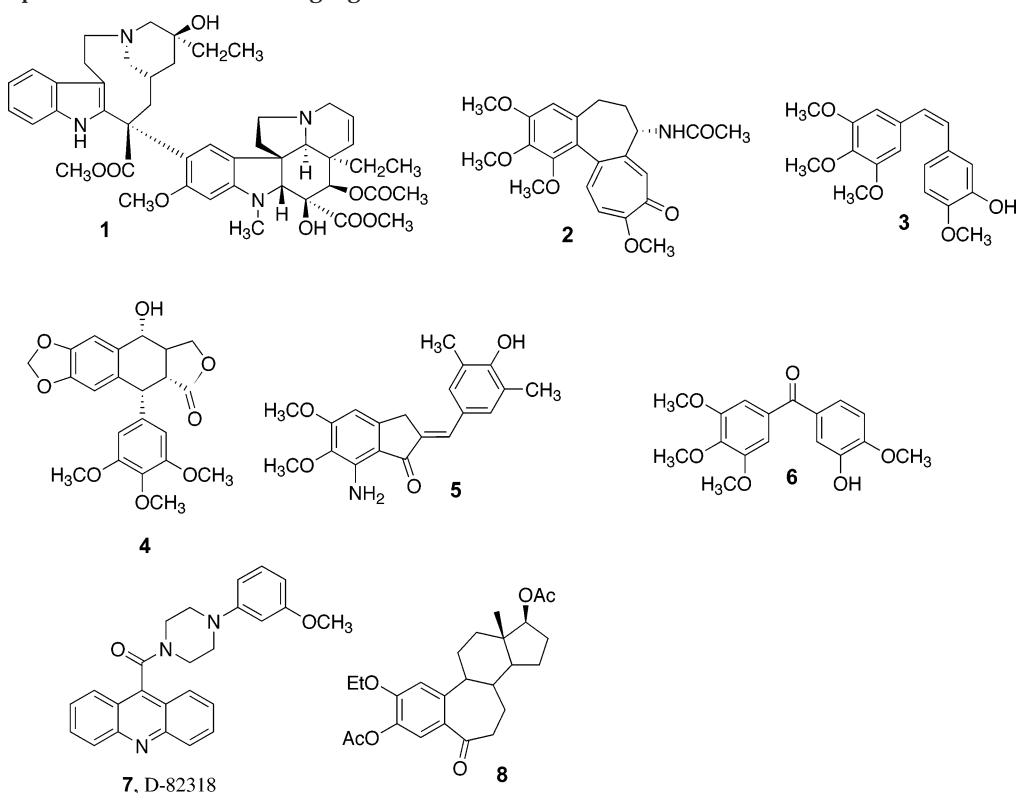
‡ Keio University.

§ Institute of Molecular Biotechnology e.V.

|| Zentaris AG.

⊥ Interdisciplinary Center for Clinical Research, Research Group "Apoptosis and Cell Death", Westphalian Wilhelms University.

⊗ Oncotest GmbH.

**Chart 1.** Examples of Tubulin Interacting Agents

tions. However, the binding site interactions for a certain number of tubulin binders are not completely known.

The vinca alkaloids, typified by vinblastine (**1**, Chart 1) and vincristine as well as the taxanes, such as taxol (INN: paclitaxel) and taxotere (INN: docetaxel), are the mostly used antimicrotubule agents for the treatment of cancer and have been successfully introduced to clinical oncology.<sup>4</sup> Colchicine (**2**) is another important antimitotic agent. Although it has limited medicinal utility due to its small therapeutic window, colchicine has played a fundamental role in elucidation of the properties and functions of tubulin and microtubules.<sup>5</sup> Additionally, the natural products combretastatin A-4<sup>6</sup> (**3**), curacin A,<sup>7</sup> podophyllotoxin<sup>8</sup> (**4**), epothilones A and B<sup>9</sup> and dolastatin<sup>10</sup> as well as some more synthetic compounds including indanocine<sup>11</sup> (**5**), phenstatin<sup>12</sup> (**6**), acridinyl-9-carboxamide D-82318<sup>13</sup> (**7**), and the 2-ethoxyestradiol analogue<sup>14</sup> (**8**) (Chart 1), to cite just a few, are known to mediate cytotoxic activities through a binding interaction with tubulin. However, no new tubulin polymerization inhibitor of low molecular weight has come into the market as yet.

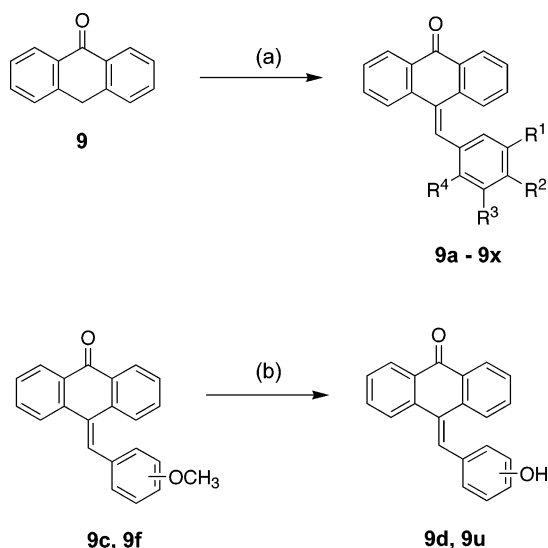
In our search for potent and selective antitumor agents, a novel series of 9(10*H*)-anthracenones bearing alkylidene- and alkyl-linked aromatic substituents in the 10-position were synthesized and assayed for anti-proliferative activity against human chronic myelogenous K562 leukemia cells. The most active inhibitors were found in the benzylidene series. For cytotoxicity, selected compounds were evaluated in the XTT assay. Furthermore, induction of cell death in a panel of tumor cell lines was measured in a monolayer assay. Several compounds strongly inhibited the growth of tumor cell lines at nanomolar concentrations, acted in a cell cycle dependent manner and induced apoptosis in cancer

cells. Additionally, they were found to be potent inhibitors of tubulin polymerization in the turbidity assay. Activities were comparable to those of the reference compounds, such as nocodazole, podophyllotoxin, and colchicine, as determined in the same assay. Herein, we report the structure–activity relationship as well as the biological data of this novel class of highly active and easily accessible antimicrotubule agents.

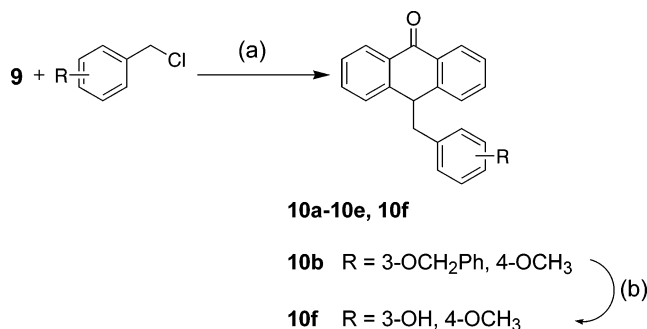
## Chemistry

Condensation reaction of 9(10*H*)-anthracenone (**9**, Scheme 1) with aldehydes is generally applicable.<sup>15</sup> The substituted benzylidene-9(10*H*)-anthracenones were obtained by a straightforward aldol-type condensation reaction of 9(10*H*)-anthracenone with appropriately substituted benzaldehydes under basic conditions in the presence of pyridine/piperidine (method A, Experimental Section).<sup>16,17</sup> In a more efficient route, gaseous hydrogen chloride was used for the condensation reaction (method B).<sup>18</sup> Acidic reaction conditions led to esterification of the carboxyaldehydes in the case of **9x**. The structural variations described here concerned the benzylidene moiety of the molecules and the conversion of some methoxy derivatives into the free phenols. The starting benzaldehydes were obtained from commercial sources or prepared according to the literature. For the preparation of compounds **9d** and **9u**, ether groups of **9c** and **9f** were cleaved by boron tribromide in dichloromethane.

The C-10-benzylated derivatives of 9(10*H*)-anthracenone (**10a–f**) were prepared as outlined in Scheme 2. Monoalkylation was achieved by reaction of 9(10*H*)-anthracenone with the corresponding benzylic chlorides in the presence of potassium carbonate in acetone.<sup>19</sup> Attempts to obtain the monoalkylated compounds by using benzylic bromides or by alkylating anthrone

**Scheme 1<sup>a</sup>**

<sup>a</sup> R<sup>1</sup>–R<sup>4</sup> are defined in Table 1. Reagents: (a) substituted benzaldehyde, acidic (gaseous HCl) or basic (pyridine/piperidine) conditions; (b) BBr<sub>3</sub>, CH<sub>2</sub>Cl<sub>2</sub>, –78 °C, N<sub>2</sub>.

**Scheme 2<sup>a</sup>**

<sup>a</sup> R is defined in Table 1. Reagents: (a) K<sub>2</sub>CO<sub>3</sub>, KI, acetone; (b) glacial acetic acid, HCl 37%, Δ, 20 min.

monoanion in aqueous alkaline solution<sup>20</sup> failed. Compound **10f** was synthesized by debenzoylation of **10b** using a mixture of glacial acetic acid and HCl.

**Biological Evaluation and Discussion**

**In Vitro Cell Growth Inhibition Assay.** The compounds were initially screened for antiproliferative activity against the human chronic myelogenous leukemia cell line K562.<sup>21</sup> Cell proliferation was determined directly by counting the cells with a Coulter counter after 48h of treatment. The structures of the benzylidene-9(10*H*)-anthracenones are listed in Table 1, together with the growth inhibitory data. The observed antiproliferative activities were obviously dependent on the substitution pattern of the benzylidene part. 10-[(3-Hydroxy-4-methoxybenzylidene)]-9(10*H*)-anthracenone **9h**, which incorporates partial structures of both combretastatin A-4 (**3**) and phenstatin (**6**, Chart 1), displayed excellent antiproliferative activity (IC<sub>50</sub> K562: 0.02 μM). It was revealed to be the most active compound in this assay, and it was found to be almost as potent as adriamycin (IC<sub>50</sub> K562: 0.01 μM). In addition, compounds **9b**, **9d**, and **9g** were also found to be highly active with IC<sub>50</sub> values < 0.1 μM. However, the structural differences between these compounds did

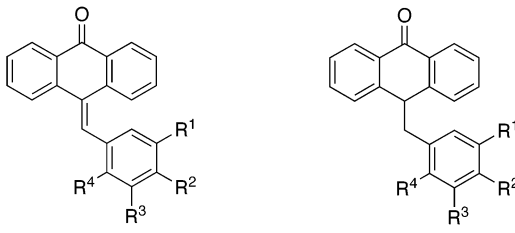
not greatly affect the antiproliferative potency, and the activity of **9h** was not improved. Noteworthy, the isomeric **9i** was determined to be 70-fold less potent than **9h** (**9i**, 1.4 μM vs 0.02 μM for **9h**), whereas activity of **9j** was found between these two compounds. Furthermore, a hydroxy group being flanked by methoxy groups in the case of **9k** and **9l** resulted in highly active compounds. Replacement of methoxy groups by bromo atoms was well tolerated and produced the highly active compound **9o** (IC<sub>50</sub> K562: 0.16 μM). Introduction of chloro (**9p**) or nitro substituents (**9w**) resulted in compounds with reduced antiproliferative activity compared with those bearing methoxy and/or hydroxy substituents. Bulky substituents were also detrimental to potency as documented by **9m** versus **9q**. The unsubstituted compound **9a** displayed modest antiproliferative activity. The bismethoxy-substituted derivatives **9c** and **9e** had IC<sub>50</sub> values of 0.6 μM each, thus being 10-fold less active than **9b** (IC<sub>50</sub> K562: 0.06 μM) but far more potent than **9f** (IC<sub>50</sub> K562: 4 μM). Interestingly, introduction of a 3,4,5-trimethoxyphenyl group in **9f**, a well-defined pharmacophore for the inhibition of tubulin polymerization found in colchicine, combretastatin A-4, and podophyllotoxin, strongly decreased growth inhibitory properties in comparison with **9b** and **9h**. The 4,5-methylenedioxy bridge compound **9r** displayed moderate activity, whereas compounds **9s**, **9u**, and **9v** were considered to be weak growth inhibitors (IC<sub>50</sub> values ≥ 20 μM).

The 10-phenylalkyl-substituted compounds revealed a dramatically decreased inhibitory effect on cell growth (**9h** vs **10f**, **9b** vs **10a**, **9c** vs **10c**), indicating the potential importance of a restricted conformational flexibility in the case of the benzylidenes. Consistent with the findings in the benzylidene series, the isovanillin derived compound **10f** was found to be the most active one within the 10-phenylalkyl series. However, its antiproliferative effect was not very pronounced.

No relationship between antiproliferative activity and lipophilicity<sup>22</sup> in the benzylidene series was observed (calculated ClogP data not shown).

**Effect on Growth of Different Tumor Cell Lines.**

To further investigate the antiproliferative potential, the effect of highly active compounds **9h** and **9l** against a panel of five tumor cell lines derived from solid tumors was measured by cellular metabolic activity using the XTT (2,3-bis-(2-methoxy-4-nitro-5-sulfophenyl)-2*H*-tetrazolium-5-carboxanilide) assay.<sup>23</sup> Both compounds were slightly more potent than nocodazole and showed excellent cytotoxicities with IC<sub>50</sub> values in the range of <0.1 μM toward several proliferating cell lines (Table 2). The compounds were not active against RKO cells (human colon adenocarcinoma) with ectopic inducible expression of cyclin-dependent kinase inhibitor p27<sup>kip1</sup>.<sup>24</sup> By contrast, growth of proliferating RKO cells was strongly inhibited by **9l** and **9h** with IC<sub>50</sub> values of 0.05 and 0.06 μM, respectively, indicating cytotoxicity toward cycling cells. One of the greatest limitations on the efficiency of cancer chemotherapy is the development of multiple drug resistance (MDR) in patients, meaning that cancer cells evade chemotherapy by developing a broad spectrum resistance to several anticancer and cytotoxic drugs.<sup>25</sup> This is mediated, among other factors, by

**Table 1.** Antiproliferative Activity of Benzylidene-9(10*H*)-anthracenones and 10-(Phenylmethyl)-9(10*H*)-anthracenones against K562 Cells and Antitubulin activities


compd	R <sup>1</sup>	R <sup>2</sup>	R <sup>3</sup>	R <sup>4</sup>	K562 IC <sub>50</sub> <sup>a</sup> [μM]	ITP <sup>b</sup> IC <sub>50</sub> [μM]
<b>9a</b>	H	H	H	H	2	4.40
<b>9b</b>	H	OCH <sub>3</sub>	H	H	0.06	0.76
<b>9c</b>	OCH <sub>3</sub>	OCH <sub>3</sub>	H	H	0.6	1.70
<b>9d</b>	OH	OH	H	H	0.06	1.80
<b>9e</b>	OCH <sub>3</sub>	H	OCH <sub>3</sub>	H	0.6	> 10
<b>9f</b>	OCH <sub>3</sub>	OCH <sub>3</sub>	OCH <sub>3</sub>	H	4	10
<b>9g</b>	H	OCH <sub>3</sub>	H	OH	0.07	1.2
<b>9h</b>	OH	OCH <sub>3</sub>	H	H	0.02	0.67
<b>9i</b>	OCH <sub>3</sub>	OH	H	H	1.40	0.63
<b>9j</b>	H	H	OCH <sub>3</sub>	OH	0.73	0.91
<b>9k</b>	OCH <sub>3</sub>	OH	OCH <sub>3</sub>	H	0.17	0.63
<b>9l</b>	H	OCH <sub>3</sub>	OH	OCH <sub>3</sub>	0.25	0.43
<b>9m</b>	CH <sub>3</sub>	OH	CH <sub>3</sub>	H	0.8	0.91
<b>9n</b>	COOCH <sub>3</sub>	OH	H	H	1.4	> 10
<b>9o</b>	Br	OH	Br	H	0.16	0.48
<b>9p</b>	Cl	H	Cl	H	6	> 10
<b>9q</b>	C(CH <sub>3</sub> ) <sub>3</sub>	OH	C(CH <sub>3</sub> ) <sub>3</sub>	H	39	ND
<b>9r</b>	OCH <sub>2</sub> O	H	H	H	0.9	ND
<b>9s</b>	H	OCH <sub>2</sub> Ph	H	H	22	> 10
<b>9t</b>	H	OH	H	H	0.8	2.5
<b>9u</b>	OH	OH	OH	H	20	> 10
<b>9v</b>	H	CF <sub>3</sub>	H	H	> 20	ND
<b>9w</b>	H	NO <sub>2</sub>	H	H	3	ND
<b>9x</b>	H	COOC <sub>2</sub> H <sub>5</sub>	H	H	0.7	ND
<b>10a</b>	H	OCH <sub>3</sub>	H	H	25	2.6
<b>10b</b>	OBz	OCH <sub>3</sub>	H	H	ND	> 10
<b>10c</b>	OCH <sub>3</sub>	OCH <sub>3</sub>	H	H	62	> 10
<b>10d</b>	OCH <sub>3</sub>	H	OCH <sub>3</sub>	H	ND	10
<b>10e</b>	OCH <sub>3</sub>	OCH <sub>3</sub>	OCH <sub>3</sub>	H	> 80	> 10
<b>10f</b>	OH	OCH <sub>3</sub>	H	H	7	2.3
colchicine					0.02	1.4
nocodazole					ND	0.76
podophyllotoxin					ND	0.35
vinblastine sulfate					0.001	0.13
adriamycin					0.01	ND

<sup>a</sup> IC<sub>50</sub>, concentration of drug required for 50% inhibition of cell growth (K562). Cells were treated with drugs for 2 days. IC<sub>50</sub> values are the means of at least three independent determinations (SD < 10%). <sup>b</sup> ITP = inhibition of tubulin polymerization; IC<sub>50</sub> values were determined after 20 min at 37 °C and represent the concentration for 50% inhibition of the maximum tubulin assembly rate.

**Table 2.** Cytotoxic Activity of **9h** and **9l** against Different Tumor Cell Lines

compd	IC <sub>50</sub> [μM]					RKOp27 <sup>Kip1</sup> (human colon adenocarcinoma)	
	KB/HeLa (cervix)	SKOV3 (ovary)	SF268 (glioma)	NCI-H460 (lung)			
					not induced	induced	
<b>9h</b>	0.09	0.05	0.05	0.07	0.06	> 9	
<b>9l</b>	0.05	0.06	0.06	0.06	0.05	> 9	
paclitaxel	0.01	0.01	0.01	0.01	0.01	> 3	
nocodazole	0.14	0.17	0.30	0.15	0.11	> 10	
colchicine	0.03	0.05	0.05	0.07	0.02	> 10	

<sup>a</sup> IC<sub>50</sub> values were determined from XTT proliferation assays after incubation with test compound for 48 h. All experiments were performed at least in two replicates (*n* = 2), and IC<sub>50</sub> data were calculated from dose–response curves by nonlinear regression analysis.

overexpression of transmembrane cellular pumps, such as the 170 kDa P-glycoprotein (pgp),<sup>26</sup> encoded by the *mdr1* gene and the 180 kDa MDR protein (MRP).<sup>27</sup> The antiproliferative activity of **9h** and **9l** against tumor cell lines with different resistance phenotypes was evaluated in an XTT-based cytotoxicity assay. As documented by the IC<sub>50</sub> data (Table 3), the cytotoxic effects of **9h** and

**9l** toward different parental tumor cell lines are retained in cell lines with various MDR resistance phenotypes. In contrast to paclitaxel and vindesine, these compounds are no substrates of pgp170.

**Effect on Cell Viability.** The active compounds **9b**, **9d**, **9h**, **9i**, **9j**, **9k**, and **9l** were further assayed for the induction of cellular death in several tumor cell lines



**Table 3.** Antiproliferative Activity of **9h** and **9l**, Paclitaxel, Nocodazole, and Vindesine against Tumor Cell Lines with Different Resistance Phenotypes (XTT assay)

compd	IC <sub>50</sub> <sup>a</sup> [μM]					
	LT12	LT12 MDR	L1210	L1210 VCR	P388	P388 ADR
<b>9h</b>	0.32	0.19	0.14	0.13	0.16	0.26
<b>9l</b>	0.12	0.09	0.05	0.07	0.08	0.11
paclitaxel	0.006	0.40	0.06	>5	0.04	>5
nocodazole	0.30	0.05	0.06	0.07	0.07	0.05
vindesine	0.001	0.26	0.02	>5	0.01	1.10

<sup>a</sup> IC<sub>50</sub> values were determined from XTT proliferation assays after incubation with test compound for 48 h. All experiments were performed at least in two replicates (*n* = 2), and IC<sub>50</sub> data were calculated from dose–response curves by nonlinear regression analysis.

(Table 4) by means of a modified propidium iodide fluorescence assay, quantifying dead cells by staining of DNA and RNA.<sup>28–30</sup> Propidium iodide does not cross intact cell membranes and enters only the nucleus of dead cells by intercalation of into DNA or RNA. Besides permanent cell lines, human tumor xenograft derived cell lines were used, reflecting the typical properties of the original patient tumor of which they were derived. Again, **9h** displayed the highest activity and strongly caused a decrease in the number of viable cells (% T/C) in all cell lines tested. In addition, compound **9l** was found to be very potent. With the exception of MCF-7 cells, activities of **9l** were comparable to adriamycin or improved.

**Induction of Morphological Change in K562 Cells.** The strong antiproliferative activity of several compounds prompted us to focus on the molecular target. Interestingly, K562 cells incubated with almost all of the benzylidenes became altered in shape (Figure 1). The morphological changes appeared to be very similar to the cellular elongations caused by treatment with vinblastine. Since vinblastine is a well-known tubulin binder, the mechanism of action of the novel agents appeared to be involved in the microtubule assembly. This hypothesis was further supported by the fact that **9b** was selected as an antimetabolic agent by means of the COMPARE algorithm.<sup>31</sup>

**Effect on Cell Cycle Progression.** Tubulin is the intracellular target of compounds such as vinblastine, colchicine, podophyllotoxin, or combretastatin A4. The vinca alkaloid vinblastine, for example, is a potent inhibitor of cell proliferation and induces arrest in the G2/M phase of the cell cycle.<sup>1,32,33</sup> In an initial experiment, we examined the effect of **9h** on cell cycle progression with propidium iodide stained K562 cells. The cells were incubated with **9h** and vinblastine sulfate for 24 h. The cell cycle dependent DNA content was

determined by flow cytometry using propidium iodide in permeabilized cells. As illustrated by the virtually congruent FACS histogram (Figure 2A), it became evident that compound **9h** accumulated cells at G2/M in the concentration of 0.3 μM. For a thorough comparison of **9h** and **9l** with known G2/M cell cycle inhibitors in a dose dependent manner, we used an established KB/HeLa (human cervical epitheloid carcinoma) cell based assay system, and the percentage of cells in G2/M phase after 24 h was plotted against different concentrations of the compounds (Figure 2B). The concentration for 50% cells arrested in G2/M phase by **9h** and **9l** was found to be in the range of 0.2 μM (**9h**, 0.206 μM; **9l**, 0.234 μM), thus being 3–4-fold higher than the concentrations determined for nocodazole (EC<sub>50</sub> 0.082 μM) or taxol (EC<sub>50</sub> 0.054 μM), respectively.

**Apoptosis Induction by 9h.** Cell cycle arrest at G2/M is often followed by DNA fragmentation and the morphological features of apoptosis.<sup>33</sup> It has been documented that compounds interfering with the microtubule dynamics promote apoptosis in cancer cells.<sup>11,34,35</sup> Therefore, we have investigated the effect of **9h** on induction of apoptosis in K562 cells in a dose and time dependent manner by using a caspase assay (Figure 3). Caspases (cysteiny-l-aspartic-acid-proteases) are crucial components of apoptotic pathways. They are responsible for most biological and morphological alterations during apoptosis,<sup>36</sup> with caspase-3 being the most prominent effector caspase. Caspase-3 like protease activity was measured by monitoring the cleavage of the fluorogenic caspase-3 specific substrate DEVD-AMC in extracts from drug treated cells. K562 cells incubated with different concentrations of **9h** for 12, 24, and 48 h showed a significant time and concentration dependent increase in caspase-3-like protease activity compared with untreated cells (Figure 3). The extent of caspase-3 like protease activity at 3 μM after 48 h was similar to that of vinblastine, which was used as a positive control. These data suggest that the benzylidene-9(10*H*)anthracenones, in addition to their antiproliferative effects, also induce apoptosis in K562 cells.

Activation of caspase-3, in response to anticancer drugs, can be triggered by the mitochondrial release of pro-apoptotic factors into the cytosol.<sup>37</sup> In response to **9h**, such a release was demonstrated in MCF-7/Casp-3 cells stably transfected with green fluorescent protein (GFP)-tagged cytochrome *c*.<sup>38</sup> Epifluorescence microscopy of untreated cells revealed a typical filamentous mitochondrial cytochrome *c*-GFP signal (Figure 4A, GFP, control) and intact nuclear morphology, as revealed by Hoechst 33258 staining. Treatment with **9h** or vinblastine induced the release of cytochrome *c*-GFP,

**Table 4.** Effect of Selected Compounds against a Panel of Human Tumor Cell Lines in the Propidium Iodide Monolayer Assay

cell line	type	IC <sub>50</sub> [μM]							adriamycin
		<b>9b</b>	<b>9d</b>	<b>9h</b>	<b>9i</b>	<b>9j</b>	<b>9k</b>	<b>9l</b>	
SF-268	ZNS	0.89	1.16	0.03	2.97	0.98	0.62	0.04	ND <sup>b</sup>
H-460	lung	0.50	<0.01	<0.01	2.36	3.33	3.09	0.15	1.72
LXF 629L	lung	0.13	0.26	<0.01	2.07	2.02	0.72	0.05	0.07
LXF 529L	lung	0.26	1.62	0.52	3.23	4.45	7.49	0.07	0.03
MCF-7	breast	0.56	0.04	<0.01	2.52	0.80	4.13	1.85	0.05
401NL	breast	0.30	0.21	<0.01	1.51	0.02	0.24	<0.01	0.01
RXF 944L	renal	0.70	0.03	<0.01	2.83	0.36	0.15	<0.01	0.06

<sup>a</sup> ND: Not determined.

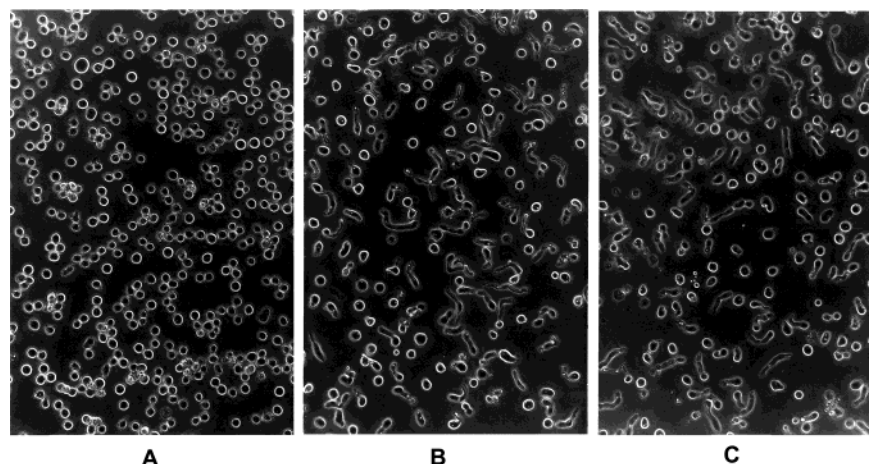


**Figure 1.** Induction of morphological change in K562 cells. K562 cells were incubated without (A), with 0.3  $\mu\text{M}$  of **9h** (B), or with 0.1  $\mu\text{M}$  of vinblastine (C) for 24 h at 37  $^{\circ}\text{C}$  and photographed under a phase-contrast microscope.

**Table 5.** Chemical Data of 10-Benzylidene-9(10*H*)-anthracenones **9a–x** and 10-(Phenylmethyl)-9(10*H*)-anthracenones **10a–f**

	formula <sup>a</sup>	method <sup>b</sup>	mp ( $^{\circ}\text{C}$ )	% yield <sup>c</sup>	solvent <sup>d</sup>	anal.
<b>9a</b>	C <sub>21</sub> H <sub>14</sub> O	A	118–120	15	MC/H (8/2)	C, H
<b>9b</b>	C <sub>22</sub> H <sub>16</sub> O <sub>2</sub>	A	144–145	49	MC	C, H
<b>9c</b>	C <sub>23</sub> H <sub>18</sub> O <sub>3</sub>	A	143–144	86	MC	C, H
		B		82		
<b>9d</b>	C <sub>21</sub> H <sub>14</sub> O <sub>3</sub>	from <b>9c</b>	204	61	EE	C, H
<b>9e</b>	C <sub>23</sub> H <sub>18</sub> O <sub>3</sub>	A	132–133	59	MC	C, H
<b>9f</b>	C <sub>24</sub> H <sub>20</sub> O <sub>4</sub>	B	176–177	55	MC/M (9.8/0.2)	C, H
<b>9g</b>	C <sub>22</sub> H <sub>16</sub> O <sub>3</sub>	A	214–216	21	MC/M (9.8/0.2)	C, H
<b>9h</b>	C <sub>22</sub> H <sub>16</sub> O <sub>3</sub>	A	144–145	38	MC/H (9/1)	C, H
		B		55		
<b>9i</b>	C <sub>22</sub> H <sub>16</sub> O <sub>3</sub>	B	199–200	18	MC	C, H
<b>9j</b>	C <sub>22</sub> H <sub>16</sub> O <sub>3</sub>	B	173–174	9	MC	C, H
<b>9k</b>	C <sub>23</sub> H <sub>18</sub> O <sub>4</sub>	B	196–198	40	MC	C, H
<b>9l</b>	C <sub>23</sub> H <sub>18</sub> O <sub>4</sub>	A	159–160	51	MC	C, H
<b>9m</b>	C <sub>23</sub> H <sub>18</sub> O <sub>2</sub>	B	183–184	77	MC	C, H
<b>9n</b>	C <sub>23</sub> H <sub>16</sub> O <sub>4</sub>	A	149–152	11	MC	C, H
<b>9o</b>	C <sub>21</sub> H <sub>12</sub> Br <sub>2</sub> O <sub>2</sub>	B	229 <sup>e</sup>	74	MC	C, H
<b>9p</b>	C <sub>21</sub> H <sub>12</sub> Cl <sub>2</sub> O <sub>2</sub>	A	163–164	49	MC	C, H
<b>9q</b>	C <sub>29</sub> H <sub>30</sub> O <sub>2</sub>	A	146–150	3	MC/H (8/2)	C, H
<b>9r</b>	C <sub>22</sub> H <sub>14</sub> O <sub>3</sub>	A	157–160	27	MC/H (7/3)	C, H
<b>9s</b>	C <sub>28</sub> H <sub>20</sub> O <sub>2</sub>	A	115–117	17	MC/H (8/2)	C, H
<b>9t</b>	C <sub>21</sub> H <sub>14</sub> O <sub>2</sub>	A	245	13	EE/PE (1/1)	C, H
<b>9u</b>	C <sub>21</sub> H <sub>14</sub> O <sub>4</sub>	from <b>9f</b>	236–239 <sup>g</sup>	71	EE	C, H
<b>9v</b>	C <sub>22</sub> H <sub>13</sub> F <sub>3</sub> O	B	121–123	65	MC	C, H
<b>9w</b>	C <sub>21</sub> H <sub>13</sub> NO <sub>3</sub>	B	181–184	75	MC	C, H
<b>9x</b>	C <sub>24</sub> H <sub>18</sub> O <sub>3</sub>	B	132	48	MC	C, H
<b>10a</b>	C <sub>22</sub> H <sub>18</sub> O <sub>2</sub>		117	30	MC	C, H
<b>10b</b>	C <sub>29</sub> H <sub>24</sub> O <sub>3</sub>		133–135	25	MC	C, H
<b>10c</b>	C <sub>23</sub> H <sub>20</sub> O <sub>3</sub>		110	31	MC	C, H
<b>10d</b>	C <sub>23</sub> H <sub>20</sub> O <sub>3</sub>		99	36	MC	C, H
<b>10e</b>	C <sub>24</sub> H <sub>22</sub> O <sub>4</sub>		112–113	34	E/PE (8/2)	C, H
<b>10f</b>	C <sub>22</sub> H <sub>18</sub> O <sub>3</sub>		95–96	28	MC	C, H

<sup>a</sup> All new compounds displayed <sup>1</sup>H NMR, FTIR, UV, and MS spectra consistent with the assigned structure. <sup>b</sup> See Experimental Section. <sup>c</sup> Yields have not been optimized. <sup>d</sup> Chromatography solvent (vol %): E = ether; EE = ethyl acetate; H = hexane; M = methanol; MC = methylene chloride; PE = petroleum ether. <sup>e</sup> Decomposition. <sup>f</sup> Elemental analyses were within  $\pm 0.4\%$  of calculated values, except where stated otherwise; <sup>g</sup>C: calcd, 76.35; found, 75.03.

indicated by a homogeneous distribution of cyt *c*-GFP (Figure 4A, arrowheads). Cells with released cyt *c*-GFP initially maintained a normal nuclear morphology, indicating that cytochrome *c* release was an upstream event. Nuclear condensation, a hallmark of apoptosis, became also evident (Figure 4A, arrows). Compound **9h** also triggered significant caspase 3-like activity in MCF-7/Casp-3 cells at a concentration of 0.3, 1, and 3  $\mu\text{M}$  (Figure 4B).

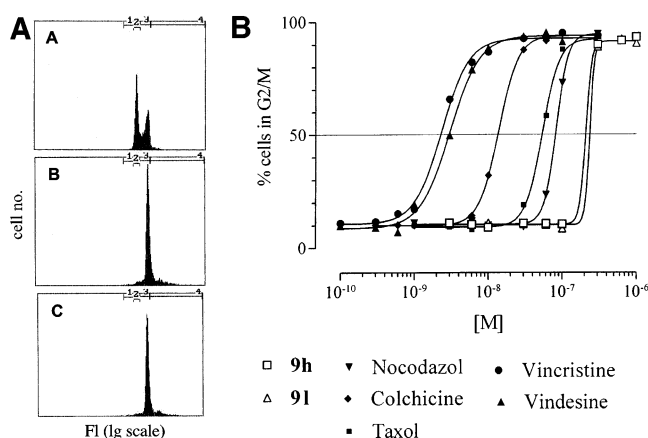


**Figure 2.** Induction of cell cycle arrest by **9h**. A, Cell cycle distribution of K562 cells showing the effect of treatment with **9h** and vinblastine sulfate (24 h assay). K562 cells were untreated (A) or treated with 0.1  $\mu\text{M}$  vinblastine (B) or 0.3  $\mu\text{M}$  of **9h** (C). Then, the cells were collected, and cell cycle distribution was measured by flow cytometry with an Epics system (Coulter Electronics, Hialeah, FL.). B, Effects of compounds **9h** and **9l** on KB/HeLa cell cycle. Subconfluent cells were exposed to different concentrations of **9h** and **9l**, nocodazole, colchicine, vincristine, or taxol for 24 h, and the percentage of cells in G2/M phase was plotted against the concentrations of the compounds.

**Western Blotting for  $\alpha$ -Tubulin.** By the cellular effects observed, we hypothesized an interaction of the benzylidenes with the microtubule system in K562 cells. Therefore, we determined the relative levels of polymerized and unpolymerized tubulin in the cells using SDS-PAGE analysis and a monoclonal  $\alpha$ -tubulin antibody. Microtubules are highly dynamic structures, also at steady-state conditions. There is constant incorporation of free dimers into the polymerized structures and release of dimers into the soluble tubulin pool. For that reason, tubulin assays performed by Western blotting are useful to determine the ratio of polymerized:unpolymerized tubulin.<sup>39,40</sup> Antimicrotubule agents such as vinblastine typically cause a shift in tubulin from the polymerized state found in the cell pellet to the unpolymerized state found in the cell supernatant. Figure 5A demonstrates the decrease in polymerized tubulin in K562 cells after treatment with compound **9h** for 24 h. Cells were harvested in the presence of a paclitaxel-stabilizing buffer, which maintains the state of micro-

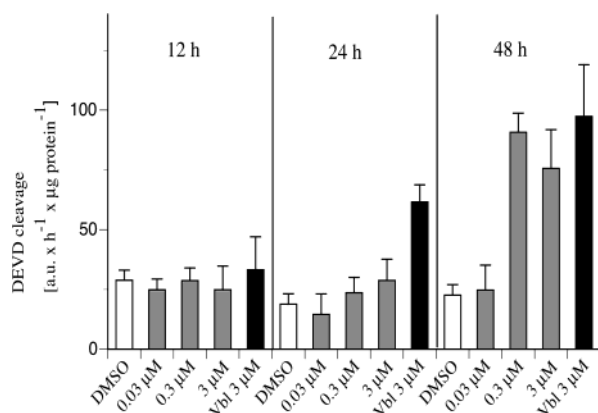


**Figure 3.** Induction of apoptosis by **9h** in K562 cells. Caspase-3-like activity was assayed in K562 cells after treatment with **9h** or vehicle. Vinblastine sulfate was used as a standard. Caspase-3-like activity is shown as cleavage rate of DEVD substrate after 12, 24, and 48 h of exposure. Cleavage of Ac-DEVD-AMC was monitored over 2 h. Data are means  $\pm$  SD from  $n = 4$  samples per treatment. A.U., arbitrary fluorescence units.

tubule assembly at the time of cell lysis.<sup>39</sup> In addition, the observed effect could also be demonstrated in a dose-dependent manner (Figure 5B).

**In Vitro Tubulin Binding Assays.** To further explore whether the growth inhibitory effect of the novel compounds was related to an interaction with the tubulin system, we evaluated them as inhibitors of tubulin polymerization. Turbidimetry, which is based upon light reflection by microtubules, provides a convenient in vitro method to preinvestigate the effect of a drug on tubulin polymerization/depolymerization. According to the temperature-dependent equilibrium between  $\alpha/\beta$ -tubulin and microtubules, assembly is observed at 37 °C while disassembly occurs by rapid cooling to 5 °C. Microtubule formation has been assayed turbidimetrically at a wavelength of 360 nm. The results obtained with the test agents are summarized in Table 1. For comparison, the data of the potent antimetabolic compounds colchicine, podophyllotoxin, nocodazole, and vinblastine are also presented. In general, drug growth inhibition correlated with the inhibition of tubulin polymerization (Figure 6), pointing to the tubulin system as a main intracellular target. The compounds with the highest antiproliferative activity were the strongest inhibitors of tubulin assembly (**9b**, **9g–i**). Most of them had  $\text{IC}_{50}$  values below 1.0  $\mu\text{M}$ , as did the reference drugs with the exception of colchicine (1.4  $\mu\text{M}$ ). The least growth inhibitory compounds had only weak inhibitory effects on tubulin polymerization ( $\text{IC}_{50}$  values ranging from 1.7 to  $>10 \mu\text{M}$ ). The compound **9h** ( $\text{IC}_{50}$  0.67  $\mu\text{M}$ ) was as antitubulin-active as podophyllotoxin. Additionally, the isomeric compounds **9i** and **9j** proved to be strongly active. The compound **9k** and the isomeric **9l** exhibited the same activity, with **9l** being the most active compound in this assay ( $\text{IC}_{50}$ : 0.43  $\mu\text{M}$ ). Compound **9b** was as good an assembly inhibitor as nocodazole, whereas a significantly reduced activity was observed for **9c** and **9f** ( $\text{IC}_{50} > 10 \mu\text{M}$ ). This was consistent with the results of the growth inhibitory assay.

It has to be pointed out that the  $\text{IC}_{50}$  values for the growth inhibitory activities and the inhibition of tubulin

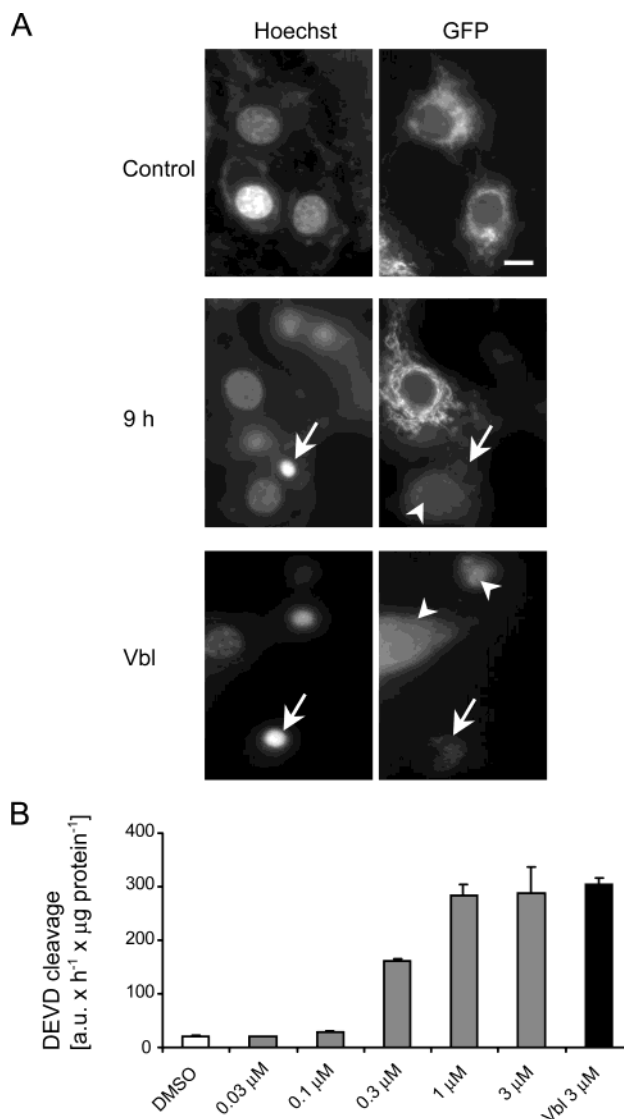


**Figure 4.** Induction of apoptosis by **9h** in MCF-7/Casp-3 cells. A, MCF-7/Casp-3 cells expressing cytochrome c-GFP were treated with **9h** or vinblastine for 36 h and stained with the chromatin specific dye Hoechst 33258. Arrowheads indicate cells with released cytochrome c-GFP. Arrows indicate cells exhibiting nuclear condensation. (Scale bar = 10  $\mu\text{M}$ ). B, Caspase-3-like activity in MCF-7/Casp-3 cells after treatment with **9h** or vehicle. Vinblastine sulfate was used as a standard. Caspase-3-like activity is shown as cleavage rate of DEVD substrate after 36 h of exposure. Cleavage of Ac-DEVD-AMC was monitored over 2 h. Data are means  $\pm$  SD from  $n = 4$  samples per treatment. A.U., arbitrary fluorescence units.

polymerization are often not in the same range. This has been repeatedly reported, and it seems to be a common feature of antimetabolic drugs.<sup>41–43</sup> It might be due to the fact that the turbidimetric measurements are performed with isolated tubulin, implicating a tubulin/benzylidene ratio different from the cellular assay using living cells. Also, additional factors such as cellular uptake, metabolism, and additional targets may exert significant effects and cannot be excluded. In consequence, by means of the tubulin assembly assay it is difficult to discriminate between highly active cell growth inhibitors ( $\text{IC}_{50} < 0.1 \mu\text{M}$ ) and those being active in the low micromolar range.

The compounds described in this report incorporate partial structures of both combretastatin A4 and phen-



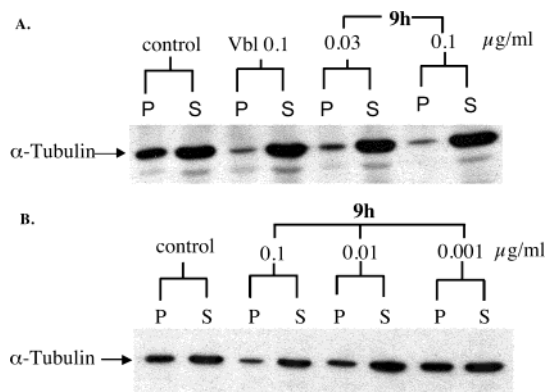


**Figure 5.** Inhibition of tubulin assembly by **9h** in K562 cells. A, K562 cells were treated with 0.1  $\mu\text{g/mL}$  and 0.03  $\mu\text{g/mL}$  of **9h** for 24 h. Vinblastine sulfate (Vbl) was used as positive control. Cells were then harvested in the presence of 4  $\mu\text{g/mL}$  paclitaxel, separated in soluble and insoluble fractions, as described in "Materials and Methods", and Western blot analysis for  $\alpha$ -tubulin was performed. Data are representative of three different experiments. P; pellet (polymerized fraction), S; supernatant (soluble fraction). B, Dose-dependent effect of **9h** on tubulin distribution in K562 cells. K562 cells were treated with 0.1, 0.01, and 0.001  $\mu\text{g/mL}$  of **9h** for 24 h. Cells were then harvested in the presence of 4  $\mu\text{g/mL}$  paclitaxel, separated in soluble and insoluble fractions, as described in Materials and Methods, and Western blot analysis for  $\alpha$ -tubulin was performed. P; pellet (polymerized fraction), S; supernatant (soluble fraction). Data are representative of three different experiments.

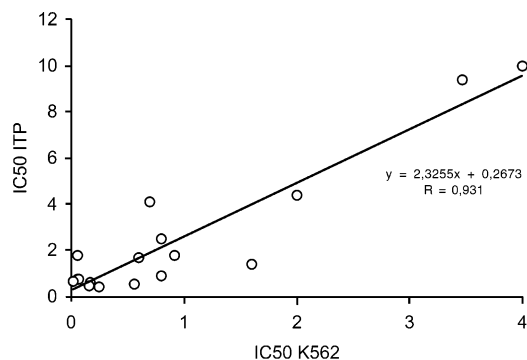


**Figure 6.** Activities of selected benzylidene-9(10*H*)-anthracenones as inhibitors of tubulin assembly compared to their activities as inhibitors of cancer cell growth.

statin, which have been demonstrated to interact with the colchicine binding site. Therefore, we tested the capability of **9h** and **9l** to compete with colchicine for binding to tubulin using a scintillation proximity assay.<sup>44</sup> Both compounds strongly displaced [<sup>3</sup>H]colchicine from its binding site (Figure 7) with exceptionally low  $\text{IC}_{50}$  values of 0.37 (**9h**) and 0.22  $\mu\text{M}$  (**9l**) versus colchicine (1.26  $\mu\text{M}$ ). No stabilization of the colchicine binding was observed, as it is documented for vinca site binders.<sup>45,46</sup> For that reason, an interaction with the colchicine binding site is highly probable whereas the binding to the vinblastine binding site appears to be unlikely.

**Electron Microscopy.** To support the former result, the effect of **9h** on microtubule assembly was compared with that of colchicine in electron microscopy (EM) studies. In the presence of 0.7  $\mu\text{M}$  of **9h**, MT assembly was inhibited (Figure 8A). A concentration near the  $\text{IC}_{50}$  allows formation of shortened microtubules, indicating

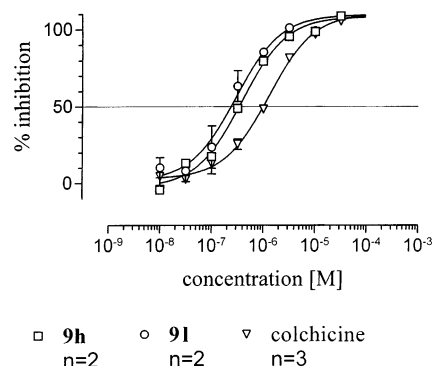


**Figure 7.** [<sup>3</sup>H]-Colchicine competition binding assay of **9h**, **9l**, and colchicine. Radiolabeled colchicine, unlabeled compound, and biotin-labeled tubulin were incubated together for 2 h at 37 °C.

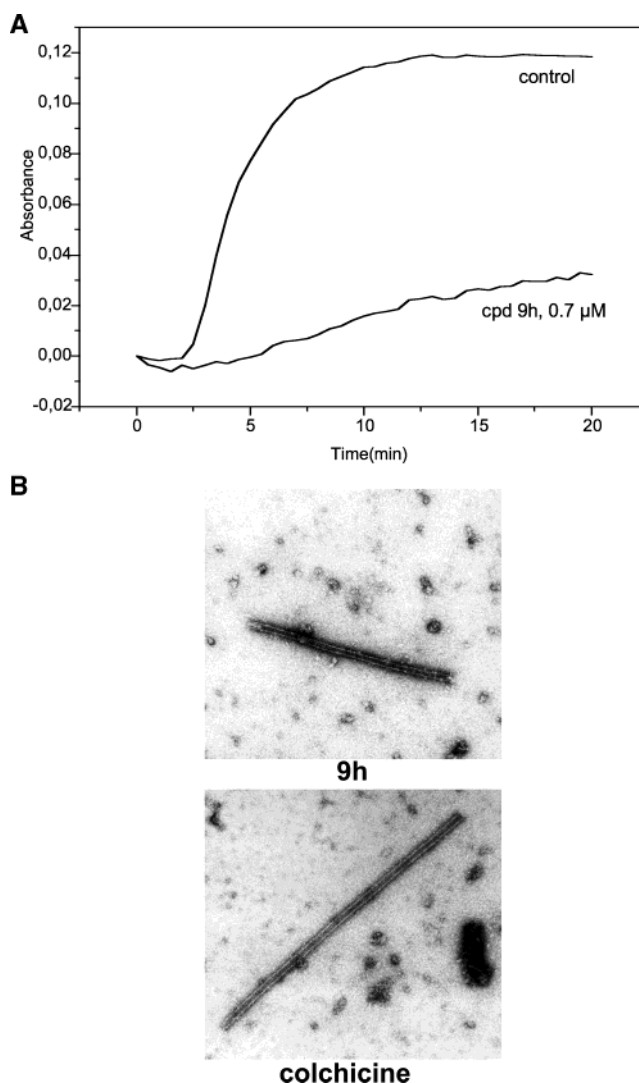


**Figure 8.** Inhibition of in vitro microtubule assembly by **9h**. A, Microtubule assembly in the presence of 0.7  $\mu\text{M}$  **9h** at 37 °C and MTP (1 mg/mL); B, Transmission electron micrographs of microtubules treated with **9h** and colchicine, negative staining by uranyl acetate. The longitudinal striation pattern is due to the protofilament substructure.

a colchicine-like effect on MT assembly (Figure 8B). Neither spiral protofilaments, being typical for a vinblastine-like effect,<sup>47</sup> nor sheetlike structures (with c-shaped profile) showing a paclitaxel-like stabilizing effect on microtubules could be detected.



## Conclusion

We have prepared several structurally novel 10-benzylidene- and 10-phenylmethyl-9(10*H*)-anthracenones. These compounds were evaluated for their antiproliferative activity against K562 cells and various other human cancer cell lines. The investigations reported in this paper were aimed at the elucidation of the mechanism of action by which these compounds exert their antiproliferative activity. As a molecular target of the compounds, we identified the tubulin system. The compounds described in this report are structurally simpler than the well-known vinblastine or the taxoids, chemically stable and easily accessible. Structure–activity relationship studies revealed that the hydroxymethoxy-substitution pattern in the benzylidene part of the molecule plays an integral role for strong growth inhibition. Several of the structurally novel benzylidene derivatives showed activities comparable to those of the strongest antiproliferative active agents and inhibitors of tubulin polymerization. Therefore, the compounds are highly attractive for further structural modifications and modeling investigations. Replacement of the benzylidene structural element by C-10-alkylation led to a distinct loss of potency in both assays. The lead compound **9h** most likely interacts with colchicine at the colchicine site, causes G2/M arrest and induces apoptotic cell death. No growth inhibitory effect was found in cell cycle arrested cells. In addition, compounds **9h** and **9l** were found to be equally potent toward parental tumor cell lines and multidrug resistant cell lines. Taken together, several compounds exhibited attractive *in vitro* antitumor activity and can therefore be considered to be potential new antimetabolic agents for further biological profiling.

Investigations to specify the interaction with the tubulin system are ongoing. Structure–activity relationship studies concerning the pharmacophore requirements for activity are in progress and should help to provide new details concerning the mechanism of action of this interesting class of antiproliferative agents.

## Experimental Section

Melting points were determined with a Kofler melting point apparatus and are uncorrected. Spectra were obtained as follows:

<sup>1</sup>H NMR spectra were recorded with a Varian Gemini 200 (50.3 MHz) or a Varian Mercury 400 plus spectrometer, using tetramethylsilane as an internal standard. Fourier transform IR spectra were recorded on a Bio-Rad laboratories Typ FTS 135 spectrometer and analysis was performed with WIN-IR Foundation software. Elemental analyses were performed at the Münster microanalysis laboratory, using a Heraeus CHN-O Rapid microanalyzer, and all values were within ±0.4% of the calculated composition. Mass spectra (EI) were recorded in the EI mode using a MAT 44S Finnigan instrument. All organic solvents were appropriately dried or purified prior to use. Aryl aldehydes were obtained from commercial sources. Analytical TLC was done on Merck silica 60 F<sub>254</sub> alumina coated plates (E. Merck, Darmstadt). Silica gel column chromatography was performed using Merck 70–230 mesh silica gel.

**General Procedure for the Preparation of 10-Benzylidene-9(10*H*)-anthracenones.** **Method A.** 9(10*H*)-Anthracenone (2.33 g, 12 mmol) and the substituted benzaldehyde (14.4 mmol) were suspended in 50 mL of dry pyridine under nitrogen. Piperidine (15 mL) was added, and the mixture was thereafter heated on an oil bath (130 °C) until the reaction was complete (TLC control). Then, the reaction

mixture was cooled to room temperature, poured on water (700 mL), and acidified with 80 mL of 6 N HCl. The precipitate was extracted with CH<sub>2</sub>Cl<sub>2</sub> (3 × 50 mL), and the organic phase was dried over Na<sub>2</sub>SO<sub>4</sub> and then concentrated *in vacuo*. Finally, the residue was purified by chromatography using silica gel.

**Method B.** 9(10*H*)-Anthracenone (1.94 g, 10 mmol) and the substituted benzaldehyde (10 mmol) were dissolved in absolute ethanol (25 mL) at room temperature. Then, the suspension was saturated with gaseous hydrogen chloride for 5 min. The mixture became dark and was thereafter heated to reflux for 1 h (TLC control). The reaction mixture was thereafter cooled to room temperature, poured on water (300 mL), and extracted with CH<sub>2</sub>Cl<sub>2</sub> or ethyl acetate (free phenols). Solvents were evaporated at reduced pressure, and the residue was purified by column chromatography using silica gel. All products were obtained as solids.

**Cleavage of Ethers with Boron Tribromide.** The substrate (0.58 mmol) is dissolved in CH<sub>2</sub>Cl<sub>2</sub> (10 mL) and cooled to –78 °C. A solution of 1 molar boron tribromide in dichloromethane (5 mL, 5 mmol) is added dropwise with stirring. The stirring is continued overnight while the mixture is allowed to warm to room temperature. Then, the reaction is terminated by addition of water (300 mL) and the product is subsequently extracted with ethyl acetate. The extract is dried with Na<sub>2</sub>SO<sub>4</sub> and the solvent is then removed *in vacuo*. The residue is then chromatographed on a column of SiO<sub>2</sub> using ethyl acetate as eluent.

**10-Benzylidene-9(10*H*)-anthracenone<sup>17,18</sup> (9a).** FTIR 1657 cm<sup>-1</sup>; <sup>1</sup>H NMR (CDCl<sub>3</sub>): δ 8.35–7.19 (m, 14H); MS *m/z* 282 (65.5). Anal. (C<sub>21</sub>H<sub>14</sub>O) C, H.

**10-[(4-Methoxybenzylidene)]-9(10*H*)-anthracenone (9b).**<sup>15,31</sup> FTIR 1654 cm<sup>-1</sup>; <sup>1</sup>H NMR (CDCl<sub>3</sub>) δ 8.31–6.82 (m, 13H), 3.83 (s, 3H); MS *m/z* 312 (100). Anal. (C<sub>22</sub>H<sub>16</sub>O<sub>2</sub>) C, H.

**10-[(3,4-Dimethoxybenzylidene)]-9(10*H*)-anthracenone (9c).** FTIR 1654 cm<sup>-1</sup>; <sup>1</sup>H NMR (CDCl<sub>3</sub>) δ 8.31–7.26 (m, 12H), 3.69 (s, 3H), 3.68 (s, 3H); MS *m/z* 342 (100). Anal. (C<sub>23</sub>H<sub>18</sub>O<sub>3</sub>) C, H.

**10-[(3,4-Dihydroxybenzylidene)]-9(10*H*)-anthracenone (9d).** FTIR 1651 cm<sup>-1</sup>; <sup>1</sup>H NMR (DMSO-*d*<sub>6</sub>) δ 8.26–8.15 (m, 3H), 7.69–7.27 (m, 6H), 6.87–6.82 (m, 3H), 6.10 (s (br), 1H), 5.65 (s (br), 1H); MS *m/z* 314 (100). Anal. (C<sub>21</sub>H<sub>14</sub>O<sub>3</sub>) C, H.

**10-[(3,5-Dimethoxybenzylidene)]-9(10*H*)-anthracenone (9e).** FTIR 1664 cm<sup>-1</sup>; <sup>1</sup>H NMR (CDCl<sub>3</sub>) δ 8.31–6.39 (m, 12H), 3.69 (s, 6H); MS *m/z* 342 (100). Anal. (C<sub>23</sub>H<sub>18</sub>O<sub>3</sub>) C, H.

**10-[(3,4,5-Trimethoxybenzylidene)]-9(10*H*)-anthracenone (9f).** FTIR 1658, 1643 cm<sup>-1</sup>; <sup>1</sup>H NMR (CDCl<sub>3</sub>) δ 8.31–7.26 (m, 9H), 6.55 (s, 2H), 3.89 (s, 3H), 3.72 (s, 6H); MS *m/z* 372 (100). Anal. (C<sub>24</sub>H<sub>20</sub>O<sub>4</sub>) C, H.

**10-[(2-Hydroxy-4-methoxybenzylidene)]-9(10*H*)-anthracenone (9g).** FTIR 3345, 1643 cm<sup>-1</sup>; <sup>1</sup>H NMR (DMSO-*d*<sub>6</sub>) δ 8.21–6.27 (m, 12H), 5.74 (s, 1H), 3.71 (s, 3H); MS *m/z* 328 (100). Anal. (C<sub>22</sub>H<sub>16</sub>O<sub>3</sub>) C, H.

**10-[(3-Hydroxy-4-methoxybenzylidene)]-9(10*H*)-anthracenone (9h).** FTIR 1654 cm<sup>-1</sup>; <sup>1</sup>H NMR (CDCl<sub>3</sub>) δ 8.30–7.26 (m, 12H), 5.61 (s, 1H), 3.89 (s, 3H); MS *m/z* 328 (100). Anal. (C<sub>22</sub>H<sub>16</sub>O<sub>3</sub>) C, H.

**10-[(4-Hydroxy-3-methoxybenzylidene)]-9(10*H*)-anthracenone<sup>15</sup> (9i).** FTIR 3399, 1651 cm<sup>-1</sup>; <sup>1</sup>H NMR (CDCl<sub>3</sub>) δ 8.29–7.29 (m, 9H), 6.90–6.79 (m, 3H), 5.74 (s, 1H), 3.69 (s, 3H); MS *m/z* 328 (100). Anal. (C<sub>22</sub>H<sub>16</sub>O<sub>3</sub>) C, H.

**10-[(2-Hydroxy-3-methoxybenzylidene)]-9(10*H*)-anthracenone (9j).** FTIR 3453, 1646 cm<sup>-1</sup>; <sup>1</sup>H NMR (CDCl<sub>3</sub>) δ 8.30–6.79 (m, 9H), 6.81–6.67 (m, 3H), 5.97 (s, 1H), 3.95 (s, 3H); MS *m/z* 328 (100). Anal. (C<sub>22</sub>H<sub>16</sub>O<sub>3</sub>) C, H.

**10-[(3,5-Dimethoxy-4-hydroxybenzylidene)]-9(10*H*)-anthracenone (9k).** FTIR 1650 cm<sup>-1</sup>; <sup>1</sup>H NMR (DMSO-*d*<sub>6</sub>) δ 8.84 (s (br), 1H), 8.16–6.73 (m, 11H), 3.35 (s, 6H); MS *m/z* 358 (100). Anal. (C<sub>23</sub>H<sub>18</sub>O<sub>4</sub>) C, H.

**10-[(2,4-Dimethoxy-3-hydroxybenzylidene)]-9(10*H*)-anthracenone (9l).** FTIR 1654 cm<sup>-1</sup>; <sup>1</sup>H NMR (CDCl<sub>3</sub>) δ

8.32–6.48 (m, 11H), 5.65 (s, 1H), 4.01 (s, 3H), 3.90 (s, 3H); MS *m/z* 358 (100). Anal. (C<sub>23</sub>H<sub>18</sub>O<sub>4</sub>) C, H.

**10-[(3,5-Dimethyl-4-hydroxybenzylidene)]-9(10*H*)-anthracenone (9m).** FTIR 1662 cm<sup>-1</sup>; <sup>1</sup>H NMR (DMSO-*d*<sub>6</sub>) δ 8.31–7.21 (m, 10H), 6.98 (s, 2H), 2.19 (s, 6H); MS *m/z* 326 (100). Anal. (C<sub>23</sub>H<sub>18</sub>O<sub>2</sub>) C, H.

**10-[(3-Carbomethoxy-4-hydroxybenzylidene)]-9(10*H*)-anthracenone (9n).** FTIR 1680, 1659 cm<sup>-1</sup>; <sup>1</sup>H NMR (CDCl<sub>3</sub>) δ 10.87 (s; 1H, OH), 8.31–6.88 (m, 12H), 3.93 (s, 3H); MS *m/z* 356 (100). Anal. (C<sub>23</sub>H<sub>16</sub>O<sub>4</sub>) C, H.

**10-[(3,5-Dibromo-4-hydroxybenzylidene)]-9(10*H*)-anthracenone (9o).** FTIR 1645 cm<sup>-1</sup>; <sup>1</sup>H NMR (DMSO-*d*<sub>6</sub>) δ 8.26–7.42 (m, 11H); MS *m/z* 456 (100). Anal. (C<sub>21</sub>H<sub>12</sub>Br<sub>2</sub>O<sub>2</sub>) C, H.

**10-[(3,5-Dichlorobenzylidene)]-9(10*H*)-anthracenone (9p).** FTIR 1662 cm<sup>-1</sup>; <sup>1</sup>H NMR (CDCl<sub>3</sub>) δ 8.31–7.18 (m, 12H); MS *m/z* 350 (100). Anal. (C<sub>21</sub>H<sub>12</sub>Cl<sub>2</sub>O) C, H.

**10-[(3,5-Bis-*tert*-butyl-4-hydroxybenzylidene)]-9(10*H*)-anthracenone (9q).** FTIR 2957, 1668 cm<sup>-1</sup>; <sup>1</sup>H NMR (CDCl<sub>3</sub>) δ 8.31–7.18 (m, 11H), 5.35 (s, 1H), 1.36 (s; 18H); MS *m/z* 410 (100). Anal. (C<sub>29</sub>H<sub>30</sub>O<sub>2</sub>) C, H.

**10-[(3,4-Methylenedioxybenzylidene)]-9(10*H*)-anthracenone<sup>15</sup> (9r).** FTIR 1646 cm<sup>-1</sup>; <sup>1</sup>H NMR (CDCl<sub>3</sub>) δ 8.31–6.75 (m, 12H), 5.99 (s; 2H); MS *m/z* 326 (100). Anal. (C<sub>22</sub>H<sub>14</sub>O<sub>3</sub>) C, H.

**10-[(4-Benzoyloxybenzylidene)]-9(10*H*)-anthracenone (9s).** FTIR 1656 cm<sup>-1</sup>; <sup>1</sup>H NMR (CDCl<sub>3</sub>) δ 8.35–6.90 (m, 18H), 5.08 (s; 2H); MS *m/z* 388 (72). Anal. (C<sub>28</sub>H<sub>20</sub>O<sub>2</sub>) C, H.

**10-[(4-Hydroxybenzylidene)]-9(10*H*)-anthracenone<sup>20</sup> (9t).** FTIR 3346, 1640 cm<sup>-1</sup>; <sup>1</sup>H NMR (DMSO-*d*<sub>6</sub>) δ 9.80 (s (br), 1H), 8.28–6.71 (m, 13H); MS *m/z* 298 (100). Anal. (C<sub>21</sub>H<sub>14</sub>O<sub>2</sub>) C, H.

**10-[(3,4,5-Trihydroxybenzylidene)]-9(10*H*)-anthracenone (9u).** FTIR 1649 cm<sup>-1</sup>; <sup>1</sup>H NMR (CDCl<sub>3</sub>, 400 MHz) δ 8.27–7.97 (m, 9H), 6.47 (s, 2H), 5.30 (s, 3H); MS *m/z* 330 (100). Anal. (C<sub>21</sub>H<sub>14</sub>O<sub>4</sub>) C, H.

**10-[(4-Trifluoromethylbenzylidene)]-9(10*H*)-anthracenone (9v).** FTIR 1660 cm<sup>-1</sup>; <sup>1</sup>H NMR (CDCl<sub>3</sub>) δ 8.32–7.22 (m, 13H); MS *m/z* 350 (100). Anal. (C<sub>22</sub>H<sub>13</sub>F<sub>3</sub>O) C, H.

**10-[(4-Nitrobenzylidene)]-9(10*H*)-anthracenone<sup>15</sup> (9w).** FTIR 1661 cm<sup>-1</sup>; <sup>1</sup>H NMR (CDCl<sub>3</sub>) δ 8.32–7.22 (m; 13H); MS *m/z* 327 (100). Anal. (C<sub>21</sub>H<sub>13</sub>NO<sub>3</sub>) C, H.

**10-[(4-Ethoxycarbonylbenzylidene)]-9(10*H*)-anthracenone (9x).** FTIR 1712, 1656 cm<sup>-1</sup>; <sup>1</sup>H NMR (CDCl<sub>3</sub>) δ 8.43–7.14 (m, 13H), 4.40 (q; 2H), 1.41 (t; 3H); MS *m/z* 354 (72). Anal. (C<sub>24</sub>H<sub>18</sub>O<sub>3</sub>) C, H.

**General Procedure for the Preparation of 10-(Phenylalkyl)-9(10*H*)-anthracenones.** 9(10*H*)-Anthracenone (**9**, 1 g, 5.15 mmol) and dry K<sub>2</sub>CO<sub>3</sub> (2 g) were suspended in absolute acetone (80 mL) under N<sub>2</sub>. Benzyl chloride (5.2 mmol) and catalytic amounts of potassium iodide (100 mg) were added, and the mixture was refluxed under nitrogen until the reaction was completed (TLC control). The reaction mixture was then cooled and poured into water (400 mL), acidified with 6 N HCl, and extracted with CH<sub>2</sub>Cl<sub>2</sub> (3 × 30 mL). The combined CH<sub>2</sub>-Cl<sub>2</sub> extracts were washed, dried over Na<sub>2</sub>SO<sub>4</sub>, and then evaporated. The residue was purified by chromatography.

**10-[(4-Methoxybenzyl)]-9(10*H*)-anthracenone (10a).** FTIR 1662 cm<sup>-1</sup>; <sup>1</sup>H NMR (CDCl<sub>3</sub>) δ 8.19–7.26 (m; 8H), 6.54, 6.30 (4H, AA'BB', *J*<sub>AB</sub> = 8.6 Hz), 4.51 (t; 1H, *J* = 5.73 Hz), 3.70 (s; 3H), 3.11 (d, 2H, *J* = 5.92 Hz). Anal. (C<sub>22</sub>H<sub>18</sub>O<sub>2</sub>) C, H.

**10-[(3-Benzoyloxy-4-methoxybenzyl)]-9(10*H*)-anthracenone (10b).** FTIR 1659, 1603 cm<sup>-1</sup>; <sup>1</sup>H NMR (CDCl<sub>3</sub>) δ 8.19–7.62 (m; 13H), 6.53–5.87 (m, 3H), 4.70 (s; 2H), 4.49 (t; 1H, *J* = 5.56 Hz), 3.77 (s, 3H), 3.07 (d, 2H, *J* = 5.74 Hz). Anal. (C<sub>29</sub>H<sub>24</sub>O<sub>3</sub>) C, H.

**10-[(3,4-Dimethoxybenzyl)]-9(10*H*)-anthracenone (10c).** FTIR 1661, 1601 cm<sup>-1</sup>; <sup>1</sup>H NMR (CDCl<sub>3</sub>) δ 8.18–7.37 (m; 8H), 6.52–5.75 (m, 3H), 4.55 (t; 1H, *J* = 5.75 Hz), 3.77 (s; 3H), 3.47 (s, 3H), 3.13 (d, 2H, *J* = 5.75 Hz). Anal. (C<sub>23</sub>H<sub>20</sub>O<sub>3</sub>) C, H.

**10-[(3,5-Dimethoxybenzyl)]-9(10*H*)-anthracenone (10d).** FTIR 1658 cm<sup>-1</sup>; <sup>1</sup>H NMR (CDCl<sub>3</sub>) δ 8.19–7.36 (m; 8H), 6.20 (t, 1H, *J* = 2.15 Hz), 5.57 (d; 2H, *J* = 2.35 Hz), 4.54 (t; 1H,

*J* = 5.86 Hz), 3.51 (s, 3H), 3.10 (d, 2H, *J* = 5.87 Hz); MS *m/z* 344 (81). Anal. (C<sub>23</sub>H<sub>20</sub>O<sub>3</sub>) C, H.

**10-[(3,4,5-Trimethoxybenzyl)]-9(10*H*)-anthracenone (10e).** FTIR 1658 cm<sup>-1</sup>; <sup>1</sup>H NMR (400 MHz, CDCl<sub>3</sub>) δ 8.16–7.40 (m; 8H), 5.48 (s, 2H), 4.57 (t; 1H, *J* = 5.66 Hz), 3.74 (s; 3H), 3.46 (s, 6H), 3.12 (d, 2H, *J* = 5.67 Hz). Anal. (C<sub>24</sub>H<sub>22</sub>O<sub>4</sub>) C, H.

**10-[(3-Hydroxy-4-methoxybenzyl)]-9(10*H*)-anthracenone (10f).** A suspension of **10b** (0.95 g, 2.27 mmol) in 15 mL of glacial acetic acid and HCl 37% (2 mL) was refluxed for 20 min. The reaction mixture was cooled, excess of water was added, and the mixture was then extracted with CH<sub>2</sub>Cl<sub>2</sub>. The CH<sub>2</sub>Cl<sub>2</sub> phase was dried and evaporated and the residue purified by chromatography to afford **10f**.

FTIR 3378, 1662 cm<sup>-1</sup>; <sup>1</sup>H NMR (400 MHz, CDCl<sub>3</sub>) δ 8.19–7.32 (m; 8H), 6.48–5.83 (m, 3H), 5.40 (s, 1H), 4.49 (t; 1H, *J* = 5.86 Hz), 3.79 (s, 3H), 3.06 (d, 2H, *J* = 5.86 Hz). Anal. (C<sub>22</sub>H<sub>18</sub>O<sub>3</sub>) C, H.

**Biological Assay Methods. Materials.** Vinblastine was obtained from Wako Pure Chemicals Industries, Ltd. Horseradish peroxidase (HRP) linked anti-mouse Ig (from sheep) was obtained from Amersham Life Science. Monoclonal anti-α-tubulin was provided by Sigma. Chemicals were dissolved in methanol/DMSO 1:1. Vinblastine sulfate was dissolved in methanol/water 1:1.

**Cells and Culture Conditions.** Human chronic myelogenous K562 leukemia cells were obtained from Dr. H. Tapiero, ICLG, Villejuif, France, and cultured in RPMI 1640 medium containing 10% fetal bovine serum (FBS), kanamycin (0.1 mg/mL), penicillin G (100 units/mL), and l-glutamine (30 mg/L) at 37 °C in 5% CO<sub>2</sub>. The mammary cancer cell line MCF-7 and cell line SF268 (central neural system carcinoma) were obtained from NCI. The cell lines LCL H460 (lung, large cell adenocarcinoma), LXFA 629L (lung, adenocarcinoma), LXFL 529L (large cell lung cancer), MAXF 401NL (papillary breast adenocarcinoma), and RXF 944L (renal hypernephroma) were established at the University of Freiburg/Oncotest GmbH, Freiburg. Human breast carcinoma MCF-7/Casp-3 cells stably transfected with caspase-3<sup>48</sup> were cultured in RPMI 1640 medium (Invitrogen, Carlsbad, CA) supplemented with penicillin (100 U/mL), streptomycin (100 μg/mL), and 10% fetal calf serum (PAA Laboratories GmbH, Cölbe, Germany).

The human tumor cell lines KB/HeLa (cervical carcinoma), SKOV3 (ovarian adenocarcinoma), NCI-H460, and L1210 (murine leukemia) were obtained from ATTC. The RKO human colon adenocarcinoma cells containing an ecdysone-inducible expression vector of p27<sup>kip1</sup> were described recently.<sup>49</sup>

The L1210<sup>CR</sup> cell line was described recently.<sup>50</sup> Rat LT12 cells and the LT12/MDR subline as well as P388 cells and the P388/Adr subline were provided by Dr. Nooter (University Hosp. Rotterdam, NL).

**Assay of Cell Growth.** K562 cells were plated at 2 × 10<sup>5</sup> cells/mL in 48 well dishes (Costar, Cambridge, MA). Untreated control wells were assigned a value of 100%. Drugs were made soluble in DMSO/methanol 1:1, and control wells received equal volumes (0.5%) of vehicle alone. To each well were added 5 μL of drug, and the final volume in the well was 500 μL. Cell numbers were counted with a Model ZM Coulter Counter (Coulter Electronics, Luton, England) after treatment with chemicals for 48 h. Each assay condition was prepared in triplicate, and the experiments were carried out three times. IC<sub>50</sub> values are the concentration at which cell growth was inhibited by 50%. To calculate the inhibition of growth, the number of cells at time 0 was first subtracted. The adjusted cell number was calculated as a percentage of the control, which was the number of cells in wells without the addition of compound.

**Cell Viability Assay.** A modified propidium iodide (PI) assay, quantifying dead cells by staining of DNA and RNA, was applied to determine activity against a human tumor cell panel.<sup>29</sup> Human tumor cells were plated in 96-well flat-bottomed microtiter plates (50 μL cell suspension, 1 × 10<sup>5</sup> or 5 × 10<sup>4</sup> cells/mL), and additionally 50 μL of culture medium was added. After a 24 h recovery, 50 μL of culture medium



containing 50  $\mu\text{g/mL}$  gentamycin was added into the six control wells, or medium containing the test drug was added to the wells. Each drug concentration was plated in triplicate. Following 3–6 days of incubation, depending on cell doubling time, culture medium was replaced by fresh medium, and 50  $\mu\text{L}$  of an aqueous PI solution (25  $\mu\text{g/mL}$ ) was added to each well. The fluorescence signal correlates with the number of dead cells. Fluorescence ( $\text{FU}_1$ ) was measured using a Millipore Cytofluor 2350 microplate reader (excitation 530 nm, emission 620 nm). Microplates were thereafter kept at  $-18^\circ\text{C}$  for 24 h, yielding a total cell kill. After thawing of the plates, followed by a second fluorescence measurement ( $\text{FU}_2$ ), the amount of viable cells was calculated by subtraction of  $\text{FU}_2$  from  $\text{FU}_1$ . Growth inhibition was expressed as treated/control  $\times 100$  (% T/C) and inhibiting concentrations were determined by plotting compound concentration versus cell viability.

**XTT Assay.** The XTT assay was used to determine proliferation by quantification of cellular metabolic activity.<sup>23</sup>  $\text{IC}_{50}$  values were obtained by nonlinear regression (Graphpad Prism). The various tumor cell lines were cultivated in microtiter plates ( $1 \times 10^3$  cells/well in 100  $\mu\text{L}$ ) and were incubated with different concentrations of cytotoxic agents for 48 h.

In RKO $p27^{\text{Kip1}}$  cells, expression of  $p27^{\text{Kip1}}$  was induced by 3  $\mu\text{M}$  ponasterone A in 24 h, leading to an arrest of these cells in the G1 phase of the division cycle. Cell cycle specific substances, such as tubulin inhibitors, are only cytotoxic if the cells are not arrested and the cell cycle is in progress. The assay is performed in 96-well plates. The cell count of induced cells is about three times higher than that of noninduced cells. RKO cells with/without  $p27^{\text{Kip1}}$  expression ( $2 \times 10^4$  cells/well induced;  $6 \times 10^3$  cells/well not induced, in 150  $\mu\text{L}$ ) were treated with the test compound for 48 h at  $37^\circ\text{C}$ . The controls are untreated cells ( $\pm$  induction). On day 1, the cells are plated ( $\pm$  ponasterone A) and incubated at  $37^\circ\text{C}$  for 24 h. On day 2, the test substance is added (control DMSO), and incubation at  $37^\circ\text{C}$  is continued for another 48 h. Thereafter, a standard XTT assay is carried out.

**Flow Cytometric Analysis of Cell-Cycle Status.** K562 cells were washed twice with phosphate-buffered saline (PBS), resuspended in 1 mL of PBS, fixed with 5 mL ice-cold 70% ethanol, and stored at  $4^\circ\text{C}$ . DNA content was then measured after staining with PI solution (0.1 mg/mL propidium iodide, 0.6% NP-40, and 2 mg/mL RNase) for 30 min. Finally, the cells were analyzed with a flow cytometer using an Epics system (Coulter Electronics Inc.) equipped with an argon-ion laser operated at a wavelength of 488 nm.

For a concentration-dependent cell cycle analysis, subconfluent KB/HeLa cells were exposed to test compounds for 24 h at  $37^\circ\text{C}$ , detached, and collected. After fixation with 70% ethanol, the DNA was simultaneously stained by propidium iodide and digested with RNase. The DNA content of cells was determined with a FACS Calibur<sup>TM</sup> cytometer (Beckton Dickinson, Heidelberg, Germany). The number of cells in G2/M phase was calculated by a cell cycle analysis software (Mod Fit LT; VERITY).  $\text{IC}_{50}$  values were calculated by nonlinear regression (GraphPad Prism).

**Assessment of Caspase Activity.** After treatment with 9h and vinblastine sulfate, the culture medium was aspirated, cells were washed three times with HBS, and extracts were prepared by treatment with 200  $\mu\text{L}$  of lysis buffer (10 mM Hepes, pH 7.4, 42 mM KCl, 5 mM  $\text{MgCl}_2$ , 1 mM phenylmethylsulfonyl fluoride, 0.1 mM EDTA, 0.1 mM EGTA, 1 mM dithiothreitol, 1  $\mu\text{g/mL}$  pepstatin A, 1  $\mu\text{g/mL}$  leupeptin, 5  $\mu\text{g/mL}$  aprotinin, 0.5% 3-(3-cholamidopropyl)dimethylammonio-1-propanesulfonate (CHAPS). Fifty microliters of this lysate was mixed with 150  $\mu\text{L}$  of reaction buffer (25 mM Hepes, 1 mM EDTA, 0.1% CHAPS, 10% sucrose, 3 mM DTT, pH 7.5). The reaction buffer was supplemented with 10  $\mu\text{M}$  of the caspase substrate acetyl-Asp-Glu-Val-Asp-aminomethylcoumarin (Ac-DEVD-AMC). Production of fluorescent AMC was monitored over 120 min using a spectrofluorometric plate reader (HTS 7000, Perkin-Elmer) (excitation wavelength 380 nm and emission wavelength 465 nm). Fluorescence of blanks

containing no cellular extracts were subtracted from the values. Protein content was determined using the Pierce Coomassie Plus Protein Assay reagent (KMF, Cologne, Germany), and the caspase activity is expressed as change in fluorescent units per microgram of protein and per hour.

**Epifluorescence Microscopy.** Cytochrome *c*-GFP-expressing cells ( $1.7 \times 10^4$  cells/dish in 150  $\mu\text{L}$  of medium) were cultivated at least for 36 h on 35-mm glass-bottom dishes (Willco BV, Amsterdam, The Netherlands) coated with poly-L-lysine to let them attach firmly. EGFP fluorescence was observed using an Eclipse TE 300 inverted microscope and a  $100\times$  oil immersion objective (Nikon, Düsseldorf, Germany) equipped with the appropriate filter sets. Digital images of equal exposure were acquired with a SPOT-2 camera using Spot software version 2.2.1 (Diagnostic Instruments, Sterling Heights, MI). To observe nuclear changes indicative of apoptosis, the chromatin-specific dye Hoechst 33258 was used. Cells were stained with 1  $\mu\text{g/mL}$  Hoechst 33258 (Sigma) in PBS at room temperature for 20 min. Hoechst staining was viewed with an Eclipse TE 300 inverted-stage fluorescence microscope.

**Tubulin Polymerization Assay.** To measure the degree of tubulin polymerization, we used a slightly modified method originally described by Minotti et al.<sup>39</sup> Cells were plated in 60 mm-diameter dishes (Costar) at a cell density of  $2 \times 10^5$  cells/mL. The total cell number was  $10^6$  cells. Cells were incubated with compounds for 24 h.

Thereafter, cells were washed twice in PBS without  $\text{Ca}^{2+}$  and  $\text{Mg}^{2+}$  and lysed in 70  $\mu\text{L}$  of hypotonic buffer [20 mM Tris-HCl (pH 6.8), 1 mM  $\text{MgCl}_2$ , 2 mM EGTA, 0.5% NP-40, 2 mM phenylmethylsulfonyl fluoride, 1 mM benzamide] containing 4  $\mu\text{g/mL}$  paclitaxel,<sup>39,40</sup> at  $37^\circ\text{C}$  in the dark. After vortex, a 60  $\mu\text{L}$  suspension from each tube was transferred to a new Eppendorf tube and corrected for protein amount (Bio-Rad Protein Assay). Aliquots of 50  $\mu\text{L}$  cell lysates were centrifuged at 14 000 rpm for 15 min at room temperature. Supernatants containing cytosolic (soluble) tubulin were carefully separated from pellets containing cytoskeleton (polymerized) tubulin. The pellets were resuspended in lysis buffer [50 mM Tris-HCl (pH 7.2), 125 mM NaCl, 0.5% NP-40, 0.1 mg/mL leupeptin, 1 mM phenylmethylsulfonyl fluoride] and vortexed vigorously. After centrifugation at 14 000 rpm for 15 min at room temperature, supernatants containing polymerized tubulin were transferred to new Eppendorf tubes. Fractions of soluble and polymerized tubulin were mixed with 22.5  $\mu\text{L}$  of 3x SDS-PAGE sample buffer [3x sample buffer: 150 mM Tris-HCl (pH 6.8), 30% (m/v) glycerol, 3% SDS, bromophenol blue 3%, 150  $\mu\text{L/mL}$  2-mercaptoethanol], heated for 5 min at  $95^\circ\text{C}$ , and analyzed by SDS-PAGE on a 9% gel. After SDS-PAGE, protein cell lysates were transferred to Hybond-P PVDF membranes, blocked with 10% nonfat dry milk powder in TBS-Tween for 1 h, followed by incubation with primary anti- $\alpha$ -tubulin antibody. Membranes were washed several times with TBS-Tween before probed with the secondary horseradish-peroxidase linked anti-mouse IgG, diluted in TBS-Tween. The substrate was then visualized by the Western blot enhanced chemiluminescent staining using ECL reagents.

**Isolation of MTP and in Vitro MT Assembly Assay by Turbidimetric Measurement.** Microtubule protein (MTP) consisting of 80 to 90% tubulin and 10 to 20% microtubule-associated proteins (MAPs) was isolated from porcine brain by two cycles of temperature-dependent disassembly ( $0^\circ\text{C}$ )/reassembly ( $37^\circ\text{C}$ ) according to the method described by Shelanski et al.<sup>51</sup> To increase the yield, the reassembly steps were performed in the presence of glycerol.<sup>52</sup> Satisfactory purity of the MTP was reached after the second cycle of assembly and disassembly. Microtubules to be used for determining antimicrotubule effector activities were prepared by in vitro self-assembly of MTP in the presence of GTP (guanosin-5'-triphosphate) and magnesium ions. The MTP concentration for assembly was 1 mg/mL (determined by the Lowry procedure using bovine serum albumin as a standard). Microtubules were assembled in a buffer solution containing 20 mM PIPES (1,4-piperazine diethane sulfonic acid,  $pK_a$  6.8), 80 mM NaCl, 0.5 mM  $\text{MgCl}_2$ , 1 mM EGTA (ethylenebis(oxyethyl-

enenitrilo)tetraacetic acid) by adding 0.25 mM GTP and by warming the samples to 37 °C. The steady state level, at which the mass of tubulin in the polymerized state shows no further increase, was usually observed by turbidity measurements after an incubation time of 20 min.

The turbidimetric measurement was carried out by spectrophotometry at 360 nm, and the temperature in the assembly/disassembly cuvette was regulated with a cryostat/thermostat combination. The tubulin effectors, dissolved in DMSO, were added to the cold MTP solution (MTP concentration 1 mg/mL, temperature 2 to 4 °C) in PIPES buffer (for composition see above) at pH 6.8. Immediately at the beginning of the measurement, the temperature was raised to 37 °C. After a gap phase, the MTP assembled into microtubule (MT), and the solution became turbid and achieved finally the steady state. To prove reversibility of the assembly, stabilization by the effectors or to discriminate the turbidity from an unspecific protein precipitation, the solution was cooled to 2 °C and kept for 5 min at this temperature, resulting in MT disassembly. The MTP solution became transparent again. If the drug binds to or interferes with tubulin, the assembly steady state level is decreased for assembly inhibitors or increased for MT stabilizers. The IC<sub>50</sub> value is defined as the concentration that causes a 50% deviation from the maximum tubulin assembly rate.

**<sup>3</sup>H Colchicine Competition-Binding Assay.**<sup>44</sup> <sup>3</sup>H-Colchicine was diluted, and biotin-labeled tubulin (T333, Cytoskeleton, Denver, CO) was reconstituted according to the manufacturers protocol. The diluted compounds and the <sup>3</sup>H-colchicine were transferred to a 96-well isoplate (PE-Wallac, Boston, MA), buffer, and the reconstituted biotin-labeled tubulin was added. After incubation, streptavidin-coated yttrium SPA beads (Amersham Pharmacia Biotech, Piscataway, NJ) were added, and the bound radioactivity was determined using a MicroBeta Trilux Microplate scintillation counter (PE-Wallac Boston, MA). IC<sub>50</sub> values were obtained by nonlinear regression (GraphPad Prism).

**Acquisition and Analysis of EM Data.** For EM studies, tubulin (1 mg/mL) with MAPs was incubated with **9h** (0.7 μM) or colchicine (1 μM) in assay buffer solution containing 20 mM PIPES (1,4-piperazine diethane sulfonic acid, pK<sub>a</sub> 6.8), 80 mM NaCl, 0.5 mM MgCl<sub>2</sub>, 1 mM EGTA (ethylenebis-(oxyethylenenitrilo)tetraacetic acid), and 0.25 mM GTP (guanosin-5'-triphosphate). The assembly was started by incubation at 37 °C and followed by turbidity measurements at 360 nm. The samples were applied to carbon mica interface, and the floating carbon films were transferred to a 2% aqueous uranyl acetate solution as a negative stain and mounted on copper grids. Electron micrographs were obtained using a Zeiss EM 902 A transmission electron microscope with an accelerating voltage of 80 kV. The samples were fixed, processed, and examined under EM at ×50 000.

**Acknowledgment.** We are grateful to Rie Onose, Antibiotics Laboratory, the Institut for Physical and Chemical Research (Riken), for having performed a flow cytometry study with K562 cells. We wish to thank Angelika Zinner, Katrin Meuser, and Christiane Schetler for excellent technical assistance.

## References

- Jordan, M. A.; Hadfield, J. A.; Lawrence, N. J.; McGown, A. T. Tubulin as a target for anticancer drugs: agents which interact with the mitotic spindle. *Med. Res. Rev.* **1998**, *18*, 259–296.
- Li, Q.; Sham, H. L.; Rosenberg, S. H. Antimitotic agents. *Annu. Rep. Med. Chem.* **1999**, *34*, 139–148.
- von Angerer, E. New inhibitors of tubulin polymerisation. *Exp. Opin. Ther. Pat.* **1999**, *9*, 1069–1081.
- Rowinsky, E. K.; Donehower, R. C. The clinical pharmacology and use of antimicrotubule agents in cancer chemotherapeutics. *Pharmacol. Ther.* **1992**, *52*, 35–84.
- Hastie, S. B. Interactions of colchicine with tubulin. *Pharmacol. Ther.* **1991**, *51*, 377–401.
- Pettit, G. R.; Singh, S. B.; Hamel, E.; Lin, C. M.; Alberts, D. S.; Garcia Kendall, D. Isolation and structure of the strong cell growth and tubulin inhibitor combretastatin A-4. *Experientia* **1989**, *45*, 209–211.
- Blokhin, A. V.; Yoo, H. D.; Gerald, R. S.; Nagle, D. G.; Gerwick, W. H.; Hamel, E. Characterization of the interaction of the marine cyanobacterial natural product curacin A with the colchicine site of tubulin and initial structure–activity studies with analogues. *Mol. Pharmacol.* **1995**, *48*, 523–531.
- Damayanthi, Y.; Lown, J. W. Podophyllotoxins: current status and recent developments. *Curr. Med. Chem.* **1998**, *5*, 205–252.
- Flörshheimer, A.; Altmann, K.-H. Epothilones and their analogues – a new class of promising microtubule inhibitors. *Expert Opin. Ther. Patents* **2001**, *11*, 951–968.
- Poncet, J. The dolastatins, a family of promising antineoplastic agents. *Curr. Pharm. Design* **1999**, *5*, 139–162.
- Leoni, L. M.; Hamel, E.; Genini, D.; Shih, H.; Carrera, C. J.; Cottam, H. B.; Carson, D. A. Indanocine, a microtubule-binding indanone and a selective inducer of apoptosis in multidrug-resistant cancer cells. *J. Natl. Cancer Inst.* **2000**, *92*, 217–222.
- Pettit, G. R.; Toki, B.; Herald, D. L.; Verdier-Pinard, P.; Boyd, M. R.; Hamel, E.; Pettit, R. K. Antineoplastic agents. 379. Synthesis of phenstatine phosphate. *J. Med. Chem.* **1998**, *41*, 1688–1695.
- Baasner, S.; Emig, P.; Gerlach, M.; Müller, G.; Paulini, K.; Schmidt, P.; Burger, A. M.; Fiebig, H.-H.; Günther, E. G. D-82318 – A novel, synthetic, low molecular weight tubulin inhibitor with potent in vivo antitumor activity. Presented at the EORTC-NCI-AACR Meeting, Frankfurt, Germany, Nov 19–22, 2002, poster 112.
- Wang, Z.; Yang, D.; Mohanakrishnan, A. K.; Fanwick, P. E.; Nampoothiri, P.; Hamel, E.; Cushman, M. Synthesis of B-ring homologated estradiol analogues that modulate tubulin polymerization and microtubule stability. *J. Med. Chem.* **2000**, *43*, 2419–2429.
- El-Shafie, S. M. M. Synthesis of 10-arylidene-9-anthrones & related compounds. *Indian J. Chem.* **1978**, *16B*, 828–830.
- Weitz, E. Über einige Anthronabkömmlinge. *Liebigs Ann. Chem.* **1919**, *418*, 29–35.
- Bergmann, E. D.; Rabinovitz, M.; Gilly, S. A ring enlargement in the 9,10-dihydroanthracene series. *Tetrahedron Suppl.* **1966**, *8*, 141–148.
- Rappoport, Z.; Apeloig, Y.; Greenblatt, J. Vinylic cations from solvolysis. 29. Solvolysis of 9-(α-bromoarylidene)anthrones as a probe to the reactivity-selectivity relationship in solvolysis reactions. *J. Am. Chem. Soc.* **1980**, *102*, 3837–3848.
- Müller, K.; Gürster, D.; Piwek, S.; Wiegrebe, W. Antipsoriatic anthrones with modulated redox properties. 1. Novel 10-substituted 1,8-dihydroxy-9(10H)-anthracenones as inhibitors of 5-lipoxygenase. *J. Med. Chem.* **1993**, *36*, 4099–4107.
- Dimmel, D. R.; Shepard, D. Regioselective alkylation of anthrahydroquinone and anthrone in water with quinonemethides and other alkylating agents. *J. Org. Chem.* **1982**, *47*, 22–29.
- Lozzio, C. B.; Lozzio, B. B. Human chronic myelogenous leukemia cell-line with positive philadelphia chromosome. *Blood* **1975**, *45*, 321–334.
- Rubenstein, S. M.; Baichwal, V.; Beckmann, H.; Clark, D. L.; Frankmoelle, W.; Roche, D.; Santha, E.; Schwender, S.; Thoolen, M.; Ye, Q.; Jaen, J. C. Hydrophilic, pro-drug analogues of T138067 are efficacious in controlling tumor growth in vivo and show a decreased ability to cross the blood brain barrier. *J. Med. Chem.* **2001**, *44*, 3599–3605.
- Scudiero, D. A.; Shoemaker, R. H.; Paull, K. D.; Monks, A.; Tierney, S.; Nofziger, T. H.; Currens, M. J.; Seniff, D.; Boyd, M. R. Evaluation of a soluble tetrazolium/formazane assay for cell growth and drug sensitivity in culture using human and other tumor cell lines. *Cancer Res.* **1988**, *48*, 4827–4833.
- Schmidt, M.; Lu, Y.; Parant, J. M.; Lozano, G.; Bacher, G.; Beckers, T.; Fan, Z. Differential roles of p21<sup>Waf1</sup> and p27<sup>Kip1</sup> in modulating chemosensitivity and their possible application in drug discovery studies. *Mol. Pharmacol.* **2001**, *60*, 900–906.
- Dumontet, C.; Sikic, B. I. Mechanism of action of and resistance to antitubulin agents: microtubule dynamics, drug transport, and cell death. *J. Clin. Oncol.* **1999**, *3*, 1061–1070.
- Fardel, O.; Lecureur, V.; Guillouzo, A. The P-glycoprotein multidrug transporter. *Gen. Pharmacol.* **1996**, *27*, 1283–1291.
- Cole, S. P.; Deeley, R. G. Multidrug resistance mediated by the ATP-binding cassette transporter protein MRP. *Bioessays* **1998**, *20*, 931–940.
- Dengler, W. A.; Schulte, J.; Berger, D. P.; Mertelmann, R.; Fiebig, H. H. Development of a propidium iodide fluorescence assay for proliferation and cytotoxicity assays. *Anti-Cancer Drugs* **1995**, *6*, 522–532.
- Roth, T.; Burger, A. M.; Dengler, W.; Willmann, H.; Fiebig, H. H. Human tumor cell lines demonstrating the characteristics of patient tumors as useful models for anticancer drug screening. *Contrib. Oncol.* **1999**, *54*, 145–156.



- (30) Mahboobi, S.; Pongratz, H.; Hufsky, H.; Hockemeyer, J.; Frieser, M.; Lyssenko, A.; Paper, D. H.; Bürgermeister, J.; Böhrer, F.-D.; Fiebig, H.-H.; Burger, A. M.; Baasner, S.; Beckers, T. Synthetic 2-aroylindole derivatives as a new class of potent tubulin-inhibitory, antimetabolic agents. *J. Med. Chem.* **2001**, *44*, 4535–4553.
- (31) Paull, K. D.; Lin, C. M.; Malspeis, L.; Hamel, E. Identification of novel antimetabolic agents acting at the tubulin level by computer-assisted evaluation of differential cytotoxicity data. *Cancer Res.* **1992**, *52*, 3892–3900.
- (32) Jordan, M. A.; Wendell, K.; Gardiner, S.; Derry, W. B.; Copp, H.; Wilson, L. Mechanism of inhibition of cell proliferation by Vinca alkaloids. *Cancer Res.* **1991**, *51*, 2212–2222.
- (33) Tashiro, E.; Simizu, S.; Takada, M.; Umezawa, K.; Imoto, M. Caspase-3 activation is not responsible for vinblastine-induced Bcl-2 phosphorylation and G2/M arrest in human small cell lung carcinoma Ms-1 cells. *Jpn. J. Cancer Res.* **1998**, *89*, 940–946.
- (34) Kondoh, M.; Usui, T.; Nishikiori, T.; Mayumi, T.; Osada, H. Apoptosis induction via microtubule disassembly by an antitumor compound, pironetin. *Biochem. J.* **1999**, *340*, 411–416.
- (35) Otani, M.; Natsume, T.; Watanabe, J. I.; Kobayashi, M.; Murakoshi, M.; Mikami, T.; Nakayama, T. T2T-1027, an antimicrotubule agent, attacks tumor vasculature and induces tumor cell death. *Jpn. J. Cancer Res.* **2000**, *91*, 837–844.
- (36) Nicholson, D. W. Caspase structure, proteolytic substrates, and function during apoptotic cell death. *Cell Death Differ.* **1999**, *6*, 1028–1042.
- (37) Zamzami, N.; Kroemer, G. The mitochondrion in apoptosis: how Pandora's box opens. *Nat. Rev. Mol. Cell Biol.* **2001**, *2*, 67–71.
- (38) Luetjens, C. M.; Kögel, D.; Reimertz, C.; Düsselmann, H.; Renz, A.; Schulze-Osthoff, K.; Nieminen, A.-L.; Poppe, M.; Prehn, J. H. M. Multiple kinetics of mitochondrial cytochrome *c* release in drug-induced apoptosis. *Mol. Pharm.* **2001**, *60*, 1008–1019.
- (39) Minotti, A. M.; Barlow, S. B.; Cabral, F. Resistance to antimetabolic drugs in Chinese hamster ovary cells correlates with changes in the level of polymerized tubulin. *J. Biol. Chem.* **1991**, *266*, 3987–3994.
- (40) Scala, S.; Wosikowski, K.; Giannakakou, P.; Valle, P.; Biedler, J. L.; Spengler, B. A.; Lucarelli, E.; Bates, S. E.; Thiele, C. J. Brain-derived neurotrophic factor protects neuroblastoma cells from vinblastine toxicity. *Cancer Res.* **1996**, *56*, 3737–3742.
- (41) Cushman, M.; Nagarathnam, D.; Gopal, D.; Chakraborti, A. K.; Lin, C. M.; Hamel, E. Synthesis and evaluation of stilbene and dihydrostilbene derivatives as potential anticancer agents that inhibit tubulin polymerization. *J. Med. Chem.* **1991**, *34*, 2579–2588.
- (42) Cushman, M.; He, H.-M.; Katzenellenbogen, J. A.; Varma, R. K.; Hamel, E.; Lin, C. M.; Ram, S.; Sachdeva, Y. P. Synthesis of analogues of 2-methoxyestradiol with enhanced inhibitory effects on tubulin polymerization and cancer cell growth. *J. Med. Chem.* **1997**, *40*, 2323–2334.
- (43) Oertel, B.; Vater, W.; Wiederhold, E.-M.; Schulze, W.; Baumgart, J.; Böhm, K. J.; Jelke, E.; Tint, I. S.; Viklicky, V.; Unger, E. Fluorenone-azomethines, a novel class of microtubule inhibitors that specifically affect cell proliferation. *Acta Histochem.* **1992**, *92*, 74–86.
- (44) Tahir, S. K.; Kovar, P.; Rosenberg, S.; Ng, S.-C. A rapid colchicine competition-binding scintillation proximity assay using biotin-labeled colchicine. *Biotechniques* **2000**, *29*, 156–160.
- (45) Bai, R. L.; Pettit, G. R.; Hamel, E. Binding of dolastatin 10 to tubulin at a distinct site for peptide antimetabolic agents near the exchangeable nucleotide and vinca alkaloid sites. *J. Biol. Chem.* **1990**, *265*, 17141–17149.
- (46) Bai, R.; Roach, M. C.; Jayaram, S. K.; Barkoczy, J.; Pettit, G. R.; Luduena, R. F.; Hamel, E. Differential effects of active isomers, segments, and analogues of dolastatin 10 on ligand interactions with tubulin. Correlation with cytotoxicity. *Biochem. Pharmacol.* **1993**, *45*, 1503–15.
- (47) Wu-Wong, J. R.; Alder, J. D.; Alder, L.; Burns, D. J.; Han, E. K.-H.; Credo, B.; Tahir, S. K.; Dayton, B. D.; Ewing, P. J.; Chiou, W. J. Identification and characterization of A-105972, an anti-neoplastic agent. *Cancer Res.* **2001**, *61*(4), 1486–1492.
- (48) Jänicke, R. U.; Sprengart, M. L.; Wati, M. R.; Porter, A. G. Caspase-3 is required for DNA fragmentation and morphological changes associated with apoptosis. *J. Biol. Chem.* **1998**, *273*, 9357–9360.
- (49) Schmidt, M.; Lu, Y.; Liu, B.; Fang, M.; Mendelsohn, J.; Fan, Z. Differential modulation of paclitaxel-mediated apoptosis by p21waf1 and p27kip1. *Oncogene* **2000**, *19*, 2423–2429.
- (50) Bacher, G.; Nickel, B.; Emig, P.; Vanhoefer, U.; Seeber, S.; Shandra, A.; Klenner, T.; Beckers, T. D-24851, a novel synthetic microtubule inhibitor, exerts curative antitumoral activity in vivo, shows efficacy toward multidrug-resistant tumor cells, and lacks neurotoxicity. *Cancer Res.* **2001**, *61*, 392–399.
- (51) Shelanski, M. L.; Gaskin, F.; Cantor, C. R. Microtubule assembly in the absence of added nucleotides. *Proc. Natl. Acad. Sci. U.S.A.* **1973**, *70*, 765–768.
- (52) Vater, W.; Boehm, K. J.; Unger, E. A simple method to obtain brain microtubule protein poor in microtubule-associated proteins. *Acta Histochem. Suppl.* **1986**, *33*, 123–129.

JM0307685